HIPPOCAMPUS, VOL. 4, NO. 5, PAGES 497–529, OCTOBER 1994

Model of Local Connectivity Patterns in CA3 and CA1 Areas of the Hippocampus

Christophe Bernard and Howard V. Wheal

Department of Physiology and Pharmacology, University of Southampton, Southampton, England

ABSTRACT

In this study we describe a model of connectivity linking the different neurons in the CA3 and CA1 areas of the young male rat hippocampus. The anatomical and electrophysiological values of the parameters used in the model were selected from the available literature. Each type of synapse was characterized by its spatial location on the dendritic tree, its weight, its probability of activation, and the ionotropic receptors involved. We have shown that the degree of convergence and divergence of inputs is highly dependent upon the type of neuron and its spatial location. The different gradients of connectivity we describe support the lamellar hypothesis from a functional point of view, even if the anatomical patterns seem diffuse. The analysis of the proportion of common afferents to a class of neurons further confirmed this point. It is suggested that the circuitry creates local coherence in terms of processing of information by establishing restricted areas where information is preferentially treated. The functional consequences and limitations of these findings are also discussed. This model is the first step in the development of a network model of the hippocampus with realistic architecture. ©1994 Wiley-Liss, Inc.

Key words: modeling, neuronal network, connectivity, synapses, information processing

INTRODUCTION

There is considerable experimental evidence which suggests that the hippocampus plays an important role in certain forms of learning and memory. Even if it is not yet possible to fully answer the question, "The hippocampus—what does it do?", there are several clues about the processes that this neuronal structure is involved in (Eichenbaum et al., 1992; Squire, 1992), such as declarative memory in humans (Squire, 1987), recognition of words (Heit et al., 1988), faces (Rolls, 1988), and spatial coordinates (O'Keefe, 1989). Another field of interest concerns its pathology in certain clinical conditions, such as temporal lobe epilepsy (Margerison and Corsellis, 1966) and Alzheimer's disease (Robbins and Kumar, 1987).

Since it is not known how information is coded in the brain (least of all how it is processed by a given neuronal network) it is tempting to use computer models to test hypothesis relating to the function of specific nuclei in the brain. Two strategies for modeling the structure of the hippocampus are commonly used:

The first of these is the connectionist approach, in which the gross morphological and functional characteristics of the system are used to model specific functions. In these artificial neural networks, neuronal automata (simple representations of biological neurons) are linked to each other by a connection that is characterized by a synaptic weight σ_{ij}. This parameter represents the ability of the connection to transmit information between neuron i and neuron j. The matrix (σ_{ij}) is called a connectivity matrix. In order to accurately perform a given task, these neural networks may be adaptative. During a learning phase the synaptic weights are modified generally using a Hebbian rule (Hebb, 1949). These networks (monolayer or multilayer) are based on classical concepts derived from the artificial neural network field (Kohonen, 1977; Hopfield, 1982, 1984; Kohonen, 1984; Rumelhart and McLelland, 1986). They have been employed to model classical conditioning (Schmajuk and DiCarlo, 1992), the formation of spatial or cognitive maps (O'Keefe, 1990; Treves et al., 1992; Schmajuk et al., 1993), declarative memory (Treves and Rolls, 1992), and long-term potentiation (Brown et al., 1989). These top down approaches are more concerned with an achievable goal than with the biological relevance of the parameters and functional rules.

The second approach, a bottom up one, uses realistic biological values and rules in order to model the electrophysiological behaviour of a limited volume of tissue in the hippocampus (Traub and Miles, 1991). The number of parameters increases exponentially as one tries to take into account the different receptor subtypes, ionic channels, together with many other parameters including the local feedforward and feedback connectivity patterns. When compared to the

Address correspondence and reprint requests to Prof. Howard Wheal, Department of Physiology and Pharmacology, University of Southampton, Bassett Crescent East, Southampton SO9 3TU, England.

top down approach, the range of variability of the different parameters (and thus the dynamics of the whole network) is considerably reduced by the boundaries imposed by the electrophysiological and anatomical data. Two levels of complexity can be distinguished. The first of these concerns the way each neuron is modeled. It is now clear that neurons are complex integrative units which can perform a wide range of computational tasks and cannot be reduced to simple linear integrative units of their inputs (McCulloch and Pitts, 1943). For example, bursting activity in neurons cannot be modeled without the use of nonlinear differential equations. This kind of neuronal activity is a fundamental property of single neurons since it may, in turn, drastically transform the behaviour of a whole network of cells (Miles and Wong, 1983). Experiments utilising the voltage-clamp technique have allowed a better characterization of the many ionic currents. As a result, realistic models of single pyramidal neurons with interesting predictive properties have emerged (Traub et al., 1991b). In this example a multicompartmental cable model based on modified Hodgkin-Huxley equations is used. The second level of complexity concerns modeling which involves a large number of interconnected neurons. Advances in computational technology have allowed the merger of models with these two levels of complexity (Traub and Miles, 1991; Ge et al., 1992, 1993; Willis et al., 1993) and have been used to simulate epileptiform activity and network oscillations in the hippocampus (Traub et al., 1992a, 1993b). Similar approaches have been used for modeling the behaviour of populations of cortical neurons (Lytton and Sejnowski, 1991).

Unfortunately, neither the electrophysiological behaviour of single cells nor their morphologically complexity are fully understood. For this reason the connectivity matrices are usually given random values, using gross anatomical and electrophysiological features. However, connectivity is a fundamental parameter controlling the dynamics of a neuronal network. This is particularly true for the cerebellar cortex, where this issue has been discussed in more detail (Ito, 1984). We believe that the use of realistic connectivity matrices in models of the hippocampus will put strong constraints on the space of states of the system. As a consequence, a better understanding of its dynamic properties should be gained.

Several research groups are interested in using computer models of the hippocampus à la Traub (Miles and Traub, 1986; Traub and Miles, 1991; Traub et al., 1987a, 1991a, 1993a,b) in order to obtain insights on intrinsic properties that can not be tackled experimentally (such as the behaviour of a whole population of cells for example).

The purpose of this paper is to propose a model of the connectivity between the different neuronal elements in areas CA3 and CA1 of the rat hippocampus. In particular, we will describe the phenomena of convergence and divergence of information in this system. On the basis of anatomical constraints only, we will show that local circuits emerge and discuss how they may be involved in the processing of incoming activity and impose boundaries on the space of states of the network.

We limited our investigation to the intrinsic connectivity in CA3 and CA1 since, first, many in vivo and in vitro experiments in the hippocampus are performed in these areas. Second, we wish to build a realistic model of a hippocampal slice in order to model epileptiform activity in area CA1 (Ge et al., 1992, 1993; Willis et al., 1993). Finally, a preliminary connectivity model of the dentate gyrus has already been described (Patton and McNaughton, 1993).

In the sections General Anatomical Considerations through CA1 Interneurons, we have tried to justify the different anatomical and electrophysiological parameters that are used to build our model, i.e., the spatial distribution of the synapses, their possible weights, and the ionotropic receptors involved. The connectivity model, the results of simulations, and a parametric study are presented in the section Connectivity Model of the Hippocampus. The main issues related to information processing are discussed in the Discussion section. All anatomical and electrophysiological data are summarized in Appendix A. The software programs used for the different simulations are described in Appendix B. We have also attempted to address several unresolved issues, the discussion of which can be found in each section.

GENERAL ANATOMICAL CONSIDERATIONS

The data we describe hereafter relate to CA3 and CA1 areas located in the mid part of the hippocampus along its longitudinal axis since computer models and in vitro experiments rarely use the special connectivity properties found in the temporal and septal ends of the hippocampus.

Most data relate to young male Wistar rats since they are the most common species and strain used in electrophysiological studies. When data were not available they were derived from that found in other strains (Sprague-Dawley) or species (guinea pig). Due to the considerable variability (Boss et al., 1987; Amaral et al., 1990; Braitenberg and Schutz, 1990) between species and/or strains [420,000 CA1 pyramidal cells in Sprague-Dawley vs. 320,000 in Wistar, for example (Boss et al., 1987)] correction factors were applied when necessary. Electrophysiological data were generalized across all strains or species.

In contrast to the classical terminology introduced by Lorente de Nó (Lorente de Nó, 1934) we adopted that used by Amaral et al. (Ishizuka et al., 1990), i.e., proximal CA3 ($CA3_c$) refers to the area located near the dentate gyrus. Distal CA3 ($CA3_a$) refers to the area located near CA1. Likewise, proximal (distal) CA1 refers to the area located near CA3 (subiculum, respectively). Due to the paucity of any data about the CA2 area and in any case its limited extent in the rat, we have assumed that it is anatomically and functionally part of distal CA3.

The terminology used in this study and the different types of neurons together with their connections are illustrated in Figure 1.

THE DIFFERENT TYPES OF NEURONS

In the hippocampus, neurons can be divided into two major classes: pyramidal and nonpyramidal (Lorente de Nó, 1934; Peters and Jones, 1984). Most excitatory contacts on pyramidal neurons are found on dendritic spines (Andersen et al., 1966), which are usually contacted by a single bouton (Westrum and Blackstad, 1962). The total dendritic length of CA1 pyramidal cells is 10 mm in guinea pig hippocampus (Blackstad, 1985). A distribution of 1 spine per micron (Wen-

zel et al., 1962; Andersen et al., 1987), when mapped onto the dendrites of the CA1 pyramidal cells, results in a total population of 10,000 spines. This density has recently been challenged and increased to 2.5–3 spines per micron (Andersen, 1990) producing a total of 25,000–30,000 spines. However, only 100–300 activated excitatory synapses seemed to be necessary for spike generation in CA1 pyramidal cells (Sayer et al., 1989; Andersen, 1990).

GABAergic neurons in the hippocampus (as in many other parts of the brain) play the crucial role of damping excitation and prevent, for example, the generation of bursting activity (Schwartzkroin and Prince, 1980; Traub et al., 1987a,b). Glutamate-decarboxylase (GAD) immunoreactivity has been found in the majority of the nonpyramidal cells (Ribak et al., 1978; Seres and Ribak, 1983). These neurons can be electrophysiologically distinguished from pyramidal cells (Schwartzkroin and Mathers, 1978; Schwartzkroin and Kunkel, 1985) and generate inhibitory postsynaptic potentials (IPSPs) in the pyramidal cells they contact (Knowles and Schwartzkroin, 1981). Golgi staining revealed many cell types (Ramón y Cajal, 1911; Lorente de Nó, 1934; Amaral, 1978). Moreover, GAD immunoreactivity has been reported to coexist with immunoreactivity for neuropeptides (Somogyi et al., 1984; Kosaka et al., 1985, 1988; Sloviter and Nilaver, 1987) and/or calcium-binding proteins (Baimbridge et al., 1982; Kosaka et al., 1987; Katsumaru et al., 1988; Sloviter, 1989; Nitsch et al., 1990; Danos et al., 1991; Miettinen et al., 1992). Despite this subclassification of interneurons, functional differences between these populations have not been clearly linked to the role of these peptides and proteins (Braun et al., 1985a,b; Kawaguchi and Hama, 1987; Kawaguchi et al., 1987; Bleakman et al., 1992; Klapstein and Colmers, 1993). For this reason we could not yet make any provision for subgroups nor did we include the excitatory nonpyramidal interneurons in the model, for which even less is known (Knowles and Schwartzkroin, 1981; Lacaille et al., 1987; Babb et al., 1988; Woodson et al., 1989).

However, the model includes the principal excitatory neurons (CA3 and CA1 pyramidal cells) as well as a variety of inhibitory interneurons (Babb et al., 1988; Woodson et al., 1989; Schwartzkroin and Mathers, 1978; Knowles and Schwartzkroin, 1981; Schwartzkroin and Kunkel, 1985; Kawaguchi and Hama, 1987, 1988; Lacaille et al., 1987; Lacaille and Schwartzkroin, 1988a,b, 1988b; Lacaille and Williams, 1990; Li et al., 1992; McBain and Dingledine, 1993). In CA3, these are the chandelier cells, the stratum radiatum, and the stratum oriens interneurons. In CA1 they are the chandelier cells, the basket cells, and the so-called O/A and L-M interneurons.

AFFERENTS TO CA1 AREA

Only two sets of CA1 afferents are considered here: the Schaffer collaterals (axonal branches from ipsilateral CA3 pyramidal cells) and the commissural fibres (axonal branches from contralateral CA3 pyramidal cells) which have an excitatory action (Andersen et al., 1971; Storm-Mathisen and Ottersen, 1984). We disregard all other inputs (Ribak et al., 1978; Leranth and Frotscher, 1987) because very little is known about their three-dimensional (3-D) organization and function. Even if they provide rather diffuse inputs, we cannot preclude an important role in modulating incoming activity, in particular the lacunosum-moleculare afferents impinging on the upper part of the dendritic tree. All neurons in CA1 receive inputs from both Schaffer and commissural pathways (Frotscher and Zimmer, 1983; Frotscher et al., 1984; Schwartzkroin and Kunkel, 1985; Nitsch et al., 1990) and synapses are usually located in the stratum radiatum and oriens (Frotscher et al., 1984). Despite slight differences (Swanson et al., 1978), the organization of the commissural/Schaffer pathway is bilateral, i.e., homologous parts of CA1 receive inputs from the same parts of CA3 in both hemispheres (Gottlieb and Cowan, 1973; Laurberg, 1979; Chan, 1992). Moreover, commissural fibres project to the same location as the Schaffer collaterals (Gottlieb and Cowan, 1973). In the model, commissural fibres are treated similarly to Schaffer collaterals, the only difference being that the cells of origin in CA3 are not present. Pyramidal cells located in mid and distal parts of CA3 field do not give rise to Schaffer collaterals proper but nevertheless send axonal branches to proximal and mid parts of the CA1 stratum oriens (Lorente de Nó, 1934; Blackstad, 1985; Ishizuka et al., 1990). As a matter of convenience these fibres are also called Schaffer collaterals since it is not known if they are functionally different.

The hypothesis of the lamellar organization of the hippocampus (Andersen et al., 1971), which has been demonstrated for mossy fibre projection (Blackstad et al., 1970; Swanson et al., 1978), has been challenged for CA3 to CA1 projections (Finch et al., 1983; Amaral and Witter, 1989) despite a lamellar-like projection described for six CA3 pyramidal cells stained with HRP (Tamamaki and Nojyo, 1991). *Phaseolus vulgaris* leucoagglutin injections in CA3 have shown clear gradients of projection along both septotemporal and transverse axes (Ishizuka et al., 1990). CA3 pyramidal cells located in the mid part along the septotemporal axis are characterized by the following properties (Fig. 2a):

1. Proximal CA3 pyramidal cells mainly project in the distal part of CA1 area in the upper part of the stratum radiatum. There is a preferential septal direction of projection with an angle of dispersion of 64° and a maximal density at 15° toward the septal pole for the most proximal CA3 pyramidal cells.
2. Mid CA3 pyramidal cells mainly project to the mid part of CA1 area in the lower part of the stratum radiatum and the upper part of the stratum oriens in both septal and temporal directions.
3. Distal CA3 pyramidal cells mainly project to the proximal part of CA1 area in the lower part of the stratum oriens in a preferential temporal direction. The angle of dispersion is −56° and the maximal density is −22° toward the temporal pole for the most distal CA3 pyramidal cells.

Recently, similar patterns of connectivity have been reported using biocytin-injected CA3 pyramidal cells (Li et al., 1993). The same study showed that a single CA3 pyramidal cells was contacting between 30,000 and 60,000 neurons in the ipsilateral hippocampus. It is also known that CA3 pyramidal cells have multiple axonal branchings seen as a bundle of parallel axons (Finch and Babb, 1981). Apart from the Schaffer collateral (Sayer et al., 1989) at least three sister collaterals can be found vertically in the stratum radiatum (Andersen, 1990). This gives a minimum of $4 \times 1.3 = 5.2$ synaptic contacts

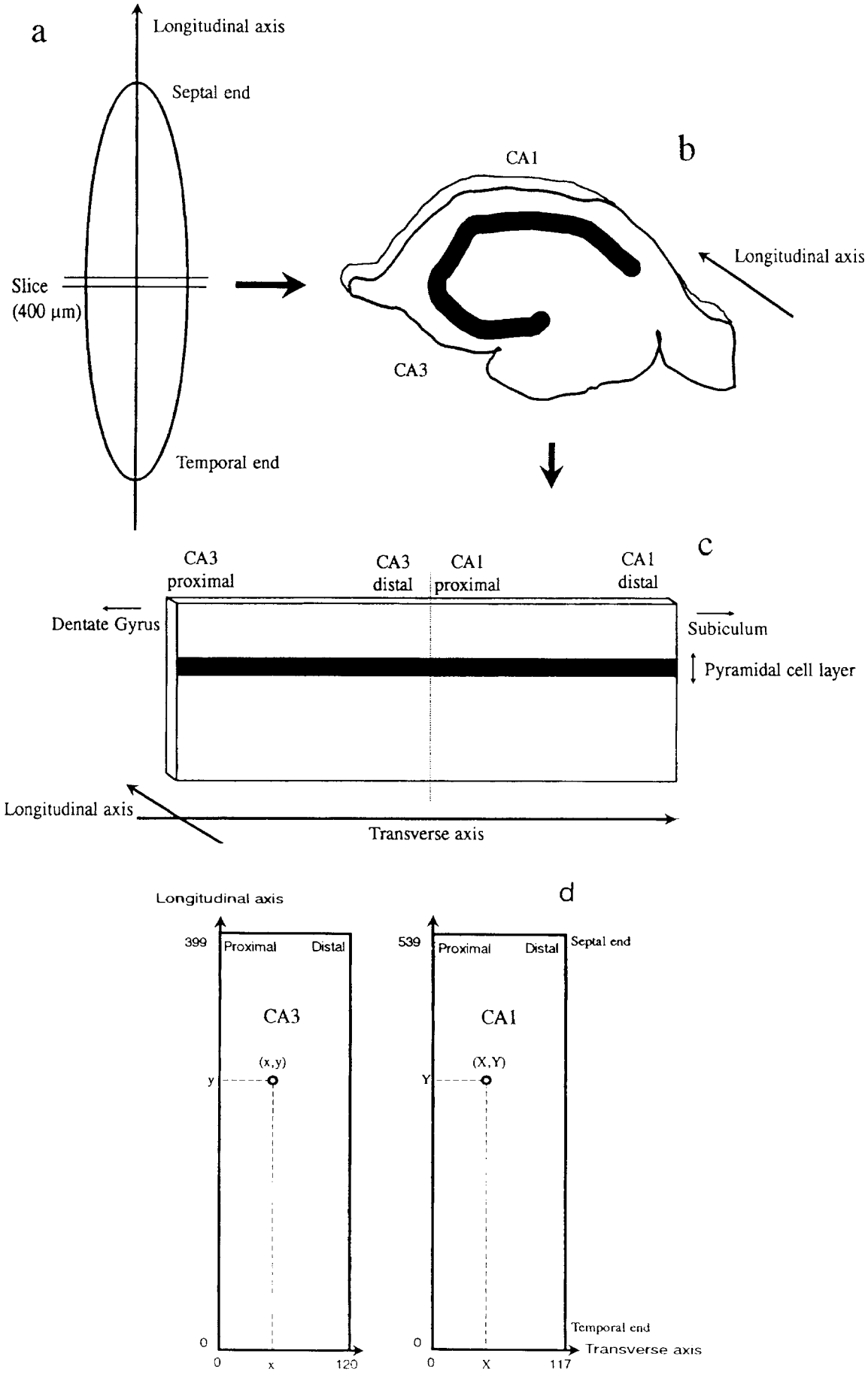
a
Longitudinal axis
Septal end
Slice
(400 μm)
Temporal end
b
CA1
CA3
Longitudinal axis
c
CA3
proximal
CA3
distal
CA1
proximal
CA1
distal
Dentate Gyrus
Subiculum
Pyramidal cell layer
Longitudinal axis
Transverse axis
d
Longitudinal axis
399
Proximal
Distal
CA3
(x,y)
y
0
0
x
120
539
Proximal
Distal
Septal end
CA1
(X,Y)
Y
0
Temporal end
Transverse axis
0
X
117

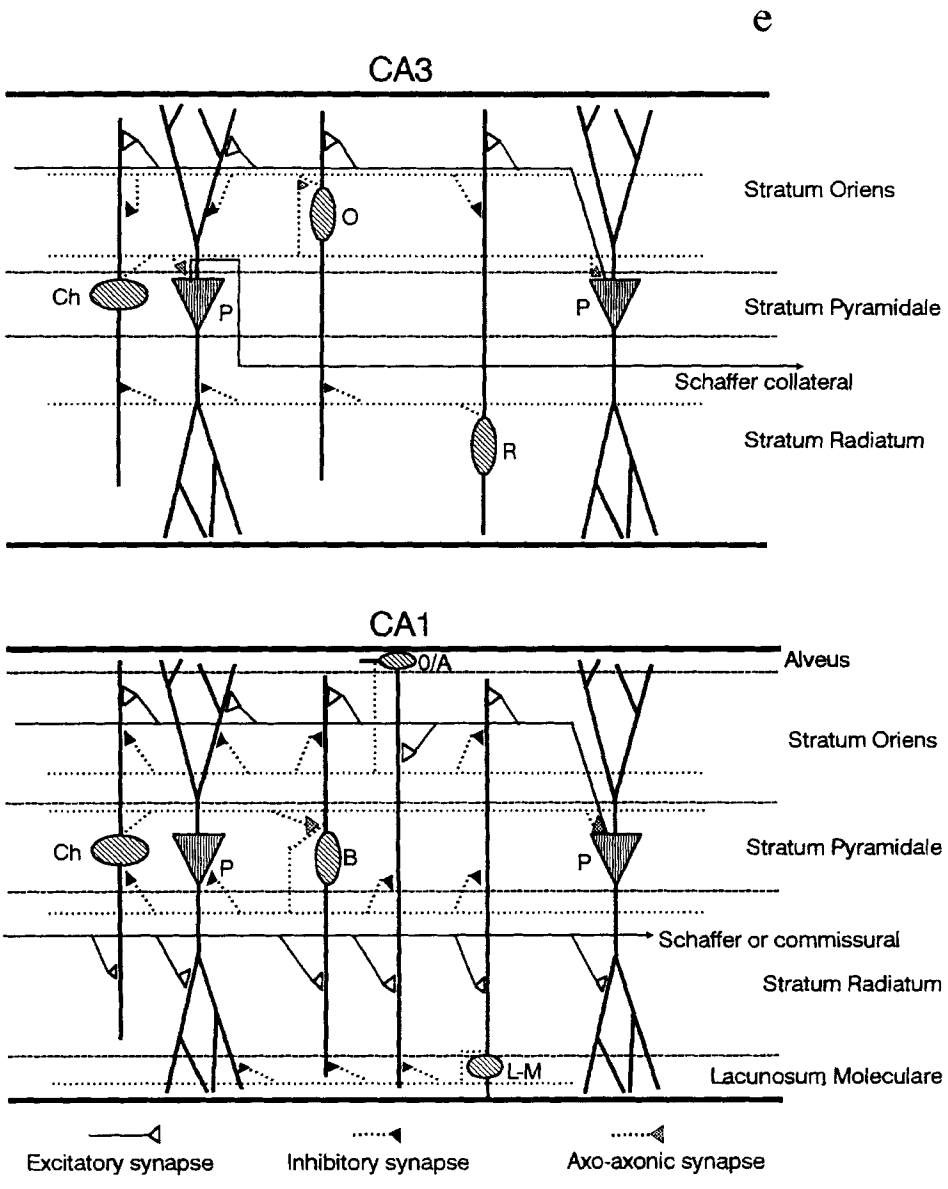

Fig. 1. **a:** View of the isolated and straightened rat hippocampus seen from above. **b:** Transverse slice of hippocampus showing CA3 and CA1 pyramidal cell layers as a thick line. **c:** Unfolded CA3 and CA1 areas from the preceding slice. The transverse and longitudinal axes and the proximal and distal regions are defined on the drawing. **d:** The unfolded and separated CA1 and CA3 areas of the hippocampus, taken from a. This shows the cell co-ordinates in each area. x=0, y=0 corresponds to the cell in CA3 located at the bottom (most temporal) left (most proximal) of the area. x=120, y=399 corresponds to the most septal and distal cell in CA3. A similar nomenclature is used in CA1 where X=0, Y=0 represents the most temporal proximal cell in the area. X=117, Y=539 corresponds to the most septal and distal cell in CA1. The number of cells along both transverse and longitudinal axes are derived from the values given in Appendix A. **e:** Simplified schematic representation of the different types of cells and their connections in CA3 and CA1 areas of the hippocampus used in this model. For the sake of clarity the CA1 and CA3 areas have been separated. P, pyramidal cell; Ch, chandelier cell; O, oriens interneuron; R, radiatum interneuron; B, basket cell; O/A, oriens/alveus interneuron; L-M, lacunosum-moleculare interneuron. Broken lines indicate the laminar boundaries. Thin continuous lines represent excitatory axonal branches. Dotted lines represent inhibitory axonal branches. Empty open triangles represent excitatory; solid triangles represent inhibitory connections; speckled triangles represent axo-axonic synapses.

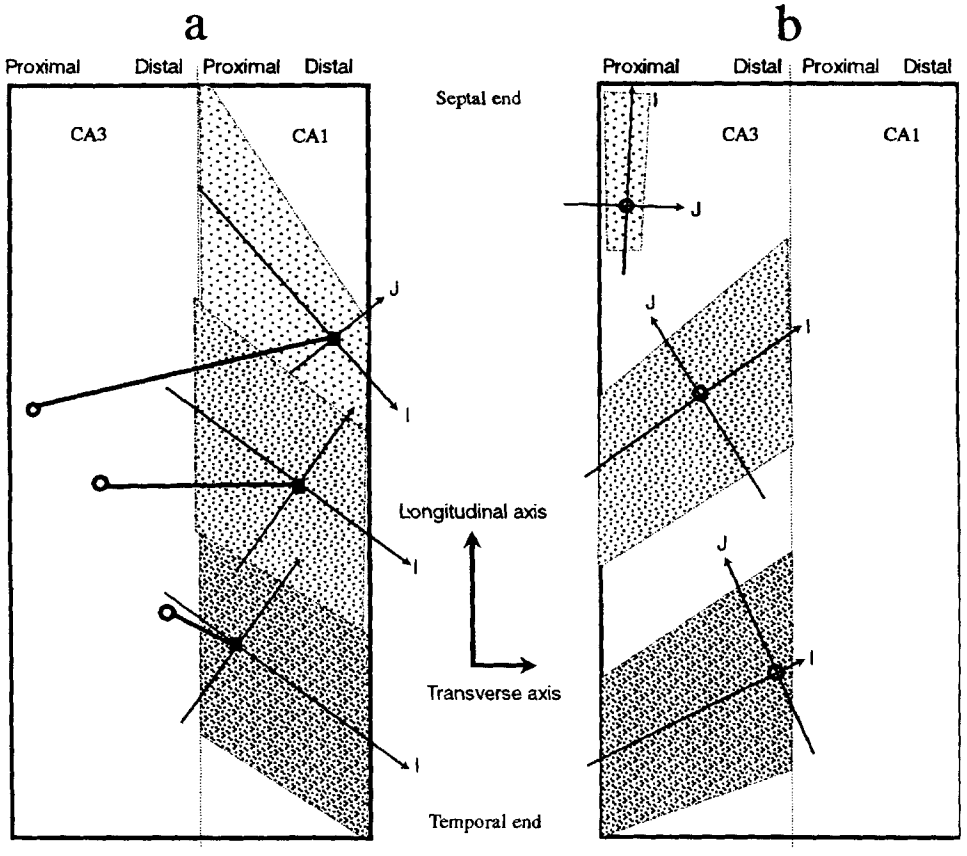

Fig. 2. **a:** Projection zones of Schaffer collaterals as a function of the location of the emitting CA3 pyramidal neurons represented by a circle. The area where the density of connections in CA1 is the highest is represented by a solid square. The patterned areas correspond to the locus of projection of the Schaffer collaterals for each proximal, mid, and distal CA3 pyramidal cells. For clarity the CA3 cells and their projection areas have been displaced along the longitudinal axis. The rules of projection relate to cells located in the middle of the hippocampus along the longitudinal axis. The distribution of connections is not uniform in each area. Following anatomical data (Ishizuka et al., 1990) we have defined two axes (I and J) along which the distribution of connections follows a simple rule. Along the I axis the density of connections decreases slowly from the area highest density (Gaussian distribution with wide dispersion). Along the J axis the density of connections decreases sharply from the area highest density (Gaussian distribution with narrow dispersion). We assume that I and J axes have the same spatial orientation for all CA3 neurons. Note that proximal neurons project to distal parts of CA1 with a preferential septal direction. Distal neurons project in proximal CA1 in a preferential temporal direction. Neurons in the mid part of CA3 project both septally and temporally. **b:** Projection zones of associational pathway as a function of the location of the emitting CA3 pyramidal neurons represented by a circle. According to anatomical data (Ishizuka et al., 1990) we also define two axes I and J along which the distribution of connections are Gaussian. Again, for clarity, each pattern is displaced along the longitudinal axis. Note that proximal neurons project locally with a preferential septal direction. Distal neurons project backward with a preferential temporal direction. Neurons in the mid part of CA3 area project forward and backward in both septal and temporal direction.

from a single CA3 pyramidal cell onto a single CA1 pyramidal cell. Moreover, single radiatum fibres have been reported to produce multiple synapses with single CA1 pyramidal cells (Sorra and Harris, 1993). This would further increase the number of synaptic contacts in CA3-CA1 pairs of pyramidal cells. However, all these synapses might not be functional since, although anatomically present, they might have a very low probability of release of neurotransmitter (Redman and Walmsley, 1983a,b). In connectionist terms this is interpreted as a null value for the synaptic weight. In models with modifiable synaptic weights these silent synapses might be switched on by relevant teaching signals.

A terminal cluster 2 mm long in the longitudinal direction and 0.4 mm long in the transverse direction has been described for a Schaffer collateral fibre (Tamamaki and Nojyo, 1991). However, a thorough description of its branching pattern was

not reported. These values are different from those reported in an earlier study (Finch et al., 1983) where the transverse extension was 1.7 mm and the longitudinal extension was 0.6 mm. Neither of these studies mention the exact location of the injected cells. The discrepancy might arise from the different gradients of connectivity within the CA3 region (Ishizuka et al., 1990). Moreover, the 2D projection makes comparison with unfolded charts difficult. However, a close inspection of the 3D reconstruction (Tamamaki and Nojyo, 1991) seems to indicate that there are gradients of connectivity similar to those reported with *Phaseolus vulgaris* leucoagglutin injections (Ishizuka et al., 1990).

As the branching pattern of Schaffer collaterals into daughter fibres is still to be elucidated, we have adopted the following model. According to the transverse location of the emitting CA3 pyramidal cell there is an area of high probability of synaptic contacts in CA1. This probability then decreases as a function of the distance. According to the pattern of projection described experimentally (Ishizuka et al. 1990), two axes (I,J) which cross at the area of maximum density of connections can be defined. Along I the density of connections decreases slowly with the distance, whereas along J it decreases sharply. We assume a Gaussian distribution with a wide dispersion along I and a peaked Gaussian distribution along J (see Figs. 2, 3). As a first approximation we consider only one synapse between an afferent fibre and a given CA1 pyramidal cell. These rules also apply to all CA1 interneurons.

Paired recordings from pyramidal cells (CA3 and CA1) in the guinea pig hippocampus have shown that the average unitary excitatory postsynaptic potential (EPSP) size is 131 μV (Sayer, 1988) with a probability of activation of the synapse of 0.1. Note that this value assumes that only one synapse is activated following stimulation of the afferent fibre. Moreover, the characteristics of the EPSP in CA1 pyramidal cell soma depend upon the spatial location of the synapse in the dendritic tree (Turner, 1988). Activation of several afferent fibres leads to a mixed synaptic response containing both NMDA and non-NMDA components (Blake et al., 1988; Collingridge et al., 1988; Andreasen et al., 1989; Hestrin et al., 1990), whereas minimal stimulation (one fibre) leads to the activation of non-NMDA receptors only (Thomson and Radpour, 1991) with an average unitary size of 120 μV (Voronin et al., 1992). NMDA and AMPA receptors are known to be colocalized at synapses in cultured rat hippocampus (Bekkers and Stevens, 1989). We may assume that this is also the case in the model with the proviso that NMDA receptors have a higher threshold for activation than that provided by the activation of a single afferent fibre. Interneurons have a larger NMDA receptor-mediated component than pyramidal cells (Capek and Esplin, 1991) and whole cell recordings showed a mixture of both AMPA and NMDA receptor-mediated components following activation of a small number of afferents (Sah et al., 1990).

In the slice, the probability of a connection between pairs of CA3 and CA1 pyramidal cells is thought to be 0.06 (Sayer et al., 1988, 1990). However, this figure should only be used in a slice model since we have seen that Schaffer collaterals have a considerable extension in the septotemporal direction (Tamamaki and Nojyo, 1991). Furthermore, the exact spatial location of these cells was not reported, and thus we have no idea whether the synaptic probability is linked to the anatomical gradients of projection.

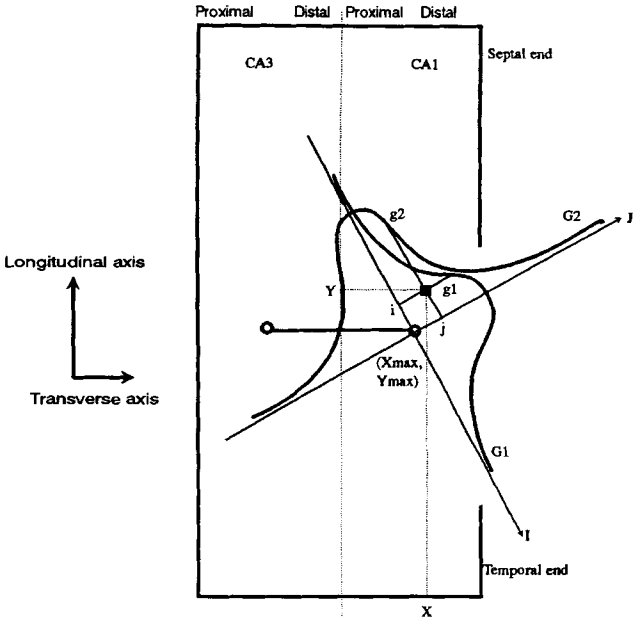

Fig. 3. Representation of the projection zone in CA1 of a given CA3 pyramidal cell. The cell is symbolized by the circle at left. The co-ordinates of the area where the highest density of connections can be found (X_{max}, Y_{max}; circle at right) was calculated following a simple linear rule. The most proximal CA3 pyramidal cell (x = 0) projects in the most distal part of CA1 (X_{max} = 117) whereas the most distal CA3 pyramidal cell (x = 120) projects to proximal CA1 (X_{max} = 0). X_{max} varies linearly with x between those boundaries. The position of Y_{max} depends upon the orientation of the projection (septal for proximal CA3 pyramidal cells, temporally for distal CA3 pyramidal cells). The projection area has an oval character (the longer, primary axis of the cloud of connections extending in the I direction and a secondary axis across in the J direction. The probability to find an axonal branch in each direction is indicated by the respective curves, G1 along I and G2 along J. Let us consider a CA1 cell with co-ordinates X,Y. In the new set of axes (I,J) which intercept at X_{max}, Y_{max}) this CA1 cell has the co-ordinates i,j. In this new system of co-ordinates X_{max} corresponds to i = 0, and Y_{max} corresponds to j = 0. We take for all i = 0, G1(0) = 1.0 and for all j = 0, G2(0) = 1.0. As a consequence the probability of finding a connection at X_{max}, Y_{max} is G1(0) × G2(0) = 1.0. For the CA1 pyramidal cell with co-ordinates (X,Y) the probability to find an axonal branch of the CA3 pyramidal cell in its vicinity is g1 × g2, where g1 = G1(i) and g2 = G2(j). If p31 is the probability of finding a connection between a given CA3 pyramidal cell and a given CA1 pyramidal cell as measured experimentally, the probability of finding a connection is g1 × g2 × p31.

Because of memory and computational speed limitations it is not reasonable to model variability in unitary responses at synapses in large-scale neuronal networks. It should be noted that the latter issue is still controversial (Raastad et al., 1992; Jonas et al., 1993). For this reason we adopted the following simplified model. The amplitude of a so-called unitary EPSP generated in the model is in fact the reflection of the synaptic weights of the given subset of synapses activated by a single

afferent fibre. The multiple contacts made by a single fibre are collapsed into a single synapse which when activated is measured as a potential at the soma. Using a multi-compartmental model of single neurons it is then possible to compute the value of the subsynaptic potential. The same considerations apply for all synapses in the model. However, when necessary two values of somatic potentials for a single synapse are given if NMDA and AMPA receptors, or $GABA_A$ and $GABA_B$ receptors, are colocalized. EPSPs and IPSPs can be approximated by either single or double exponentials (Johnston and Spruston, 1992). The probability of activation of a given synapse is also a parameter of the model.

The Schaffer/commissural pathway may be seen as a distribution line for incoming signals. As a result, its conduction velocity is a fundamentally important parameter for information processing as reported in the cerebellum for parallel fibres (Bernard and Axelrad, 1991). No systematic study has been performed to analyse possible differences in conduction velocity related to the spatial location of the emitting neurons. This is an important issue since proximal CA1 pyramidal cells will receive information before distal ones, and information is vanishing distally because of the termination gradient of incoming fibres if we assume a single conduction velocity. Any differences in conduction velocity might drastically affect the dynamics of the network. We have adopted a conduction velocity of 0.5 m/s for the Schaffer collateral pathway and 3.0 m/s for the commissural pathway (Finnerty and Jefferys, 1993). The latter values were obtained in vivo and are comparable with those obtained in vitro (Andersen et al., 1978; Grinvald et al., 1982; Knowles et al., 1987).

CONNECTIVITY BETWEEN CA3 PYRAMIDAL CELLS AND CA3 NEURONS (ASSOCIATIONAL PATHWAY)

Each CA3 pyramidal cell gives rise to three to eight primary axonal collaterals which in turn arborize to up to 40 branches (Ishizuka et al., 1990). As for the Schaffer/commissural pathway a spatial gradient of connectivity has been described (Swanson et al., 1978; Ishizuka et al., 1990).

Proximal CA3 pyramidal cells projection zone is limited: local in the transverse direction and extensive in the septal direction (ratio 3:1). A full reconstruction of a CA3 pyramidal cell filled with HRP shows an extension of 4.5 mm in the septal direction and 1.5 mm in the temporal direction (Tamamaki and Nojyo, 1991). Synapses are mainly located in stratum radiatum and oriens. Near the emitting cell the collaterals innervate both areas; more distally in the septal direction the fibres terminate in the stratum radiatum, whereas in the temporal direction the main projection zone is found in the stratum oriens (Ishizuka et al., 1990; Tamamaki and Nojyo, 1991). CA3 pyramidal cells located in the mid part of CA3 field provide associational fibres to the whole transverse extent, giving rise to most of the associational fibres per se. The fibres terminate predominantly in the stratum radiatum in both septal and temporal directions. Distal CA3 pyramidal cells project backward toward proximal and mid CA3. They innervate predominantly the stratum oriens with a preferential temporal direction. As a general property the projection zone of all CA3 pyramidal cells is more extensive in the septal direction than in the temporal one. These patterns are similar to those recently reported following injection of biocytin in CA3 pyramidal cells (Li et al., 1993). The pattern of connectivity is illustrated in Figure 2b.

In transverse slices the probability of coupling between two CA3 pyramidal cells has been reported to be 0.02 (MacVicar and Dudek, 1980; Miles and Traub, 1986). As previously stated the connections are more extensive along the septotemporal axis. Moreover, fibres in the slice might have been cut and might prevent functional connections. In a model of a transverse slice the 0.02 figure can be used, but we expect higher values in the longitudinal direction. We must stress that this 0.02 figure corresponds to the probability of finding a responsive synapse. A study based on the number of synaptic terminals in the associational pathway leads to a connectivity of 0.15 (Miles, personal communication). One of two hypothesis might explain such a discrepancy: nonfunctional synapses might exist, or small EPSPs might be masked by ongoing inhibition. The mean amplitude of the EPSP is much larger than that measured at the Schaffer collateral/CA1 pyramidal cell synapse, 1.4 mV compared to 150 μV (Miles and Traub, 1986; Williams and Johnston, 1991). These synapses also have a greater probability of transmission, 0.85 (Miles, 1990), and are very effective when inhibition is suppressed (Miles and Wong, 1987). However, in more recent recordings, it seems that the mean amplitude of associational pathway EPSP is 0.8 mV (Miles, personal communication). Intracellular recordings seem to indicate a long-duration component which might be due to the activation of NMDA receptors as described for the CA1 associational pathway (Miles and Traub, 1986; Thomson and Radpour, 1991). Moreover, active voltage-dependent dendritic currents might contribute to the overall response (Miles and Traub, 1986; Williams and Johnston, 1991).

EPSPs produced by pyramidal cell discharges on interneurons have an averaged amplitude of 1.9 mV with a high transmission probability, 0.85, and a probability of finding such connections of 0.1 (Miles, 1990; Traub and Miles, 1991). These EPSPs seem to be the result of the sole activation of non-NMDA receptors (Miles, 1990) in stratum oriens interneurons. Two types of stratum radiatum interneurons have been described (McBain and Dingledine, 1993): 75% of the total population has both AMPA (80%) and NMDA (20%) receptors and the other 25% have receptors giving an inward rectifying current. Excitatory synapses seem to be located close to the soma of the inhibitory interneurons and once activated have a high probability of discharge, 0.4 (Miles, 1990). However, recent data also suggest the presence of excitatory synapses on the distal dendrites of inhibitory interneurons (Miles, personal communication).

Finally, a reasonable estimate of the conduction velocity in the associational pathway seems to be 0.5 m/s, since the latency between the action potential and EPSP in paired recordings suggests that these fibres are unlikely to be myelinated (Miles, 1990).

CA3 INTERNEURONS

Interneurons in area CA3 are less well characterized both anatomically and functionally than those in CA1 and show various immunocytochemical reactivity (Katsumaru et al., 1988; Danos et al., 1991). Twenty-five percent of the parvalbumin-immunoreactive neurons are located in the stratum oriens, 50% are in the stratum pyramidale (of which 29% are

believed to be chandelier cells), and 25% are in the stratum radiatum (Best et al., 1993a). Because of the scarcity of data, we will consider three populations of interneurons in CA3 (Danos et al., 1991): the chandelier cells, the stratum oriens interneurons with numerous perisomatic inputs (resembling basket cells), and the stratum lucidum/radiatum interneurons with sparse perisomatic inputs. It must be kept in mind that many more types of interneurons can be found in area CA3 (at least ten, Miles, personal communication). Recently, spiny nonpyramidal cells have been described in area CA3 (Soriano and Frotscher, 1993). These interneurons are immunoreactive to glutamate but not to GABA. Since they have a widespread dendritic arborization such excitatory interneurons may play an important role in the processing of ongoing information. Unfortunately their axonal arborization is not known and so we have not included them in our model.

Excitatory synapses are located on the soma and proximal dendrites of inhibitory cells (Frotscher and Zimmer, 1983; Seres and Ribak, 1983; Frotscher et al., 1984; Schwartzkroin and Kunkel, 1985; Lang and Frotscher, 1990).

CA3 chandelier cells

Chandelier cells are known to exist in the hippocampus of mammals (Somogyi et al., 1983, 1985) and to be immunoreactive for GABA (Somogyi et al., 1985). Recently, one chandelier cell in CA1 area was completely filled with HRP (Li et al., 1992), but there is no clear evidence of their existence in CA3. However, synaptic terminals can be found on the initial segment of CA3 pyramidal cells (Kosaka, 1980) and after intracerebroventricular injection of kainic acid a population of parvalbumin-reactive neurons survive in the stratum pyramidale which may correspond to CA3 chandelier cells (Best et al., 1993b). Since data about CA3 chandelier cells are not available, we derived their properties from those found in CA1. We suppose that the dendritic arborization is contained in an ellipse with the principle axis 0.85 mm along the longitudinal direction and the small axis 0.6 mm along the transverse one. With the figures listed in the text of Appendix A we calculated a probability of 0.29 for the connection between a CA3 chandelier cell and a given CA3 pyramidal cell. A computer model of the visual cortex proposed that their role would be to increase the discharge threshold of pyramidal cells (Douglas and Martin, 1990; Lytton and Sejnowski, 1991). Given the number of synapses made on the initial segment, i.e., 100–200 (Kosaka, 1980) for five chandelier cells contacting one pyramidal cell (Best et al., 1993a), we propose that their role is also to block all eventual spike activity in the postsynaptic cell during a certain time window. Finally, the activation of chandelier cells seem to give rise to an IPSP in the soma of the neurons they contact (Miles, personal communication).

CA3 stratum oriens interneurons

Stratum oriens interneurons are fast spiking cells with a main dendritic arborization extending in the stratum oriens and a widespread axonal arborization in all strata (Kawaguchi et al., 1987). Gross measurements indicate an extension of the axonal arborization of at least 300 μm in both transverse directions. The longitudinal extension is not known. We have assumed that they have an ellipsoidal spread. The probability of connection between a stratum oriens interneuron and a given CA3 pyramidal cell is 0.6. There is no failure of synaptic transmission, and the peak amplitude of the IPSP varies between 0.6 and 4.2 mV with an average of 2.2 mV; synapses are located on or near the soma (Miles and Wong, 1984; Traub and Miles, 1991). The IPSP does not show a late component and seems to be the result of the activation of $GABA_A$ receptors only (Miles and Wong, 1984). Gap junctions are known to exist between hippocampal inhibitory cells (Katsumaru et al., 1988), but the functional consequences of these are not known (Miles, 1990). Furthermore, it is not known whether interneurons inhibit each other, but this may well be the case (Miles, personal communication). However, in the cerebellar cortex, for example, such recurrent inhibitory pathways are known to exist (Ito, 1984). In our model we have included inhibitory connections between interneurons.

CA3 stratum radiatum interneurons

Even less data are available about interneurons in stratum radiatum. We suppose that they have the same dendritic and axonal arborization as those in stratum oriens. Since a population of stratum radiatum interneurons was used for electrophysiological characterization described in the previous section we have included the same values (Miles and Wong, 1984). However, a recent study (McBain and Dingledine, 1993) on neonatal rats shows that two types of interneurons, indistinguishable anatomically but functionally different, are present in CA3 stratum radiatum. The difference lies in the absence of any NMDA component in a small subset of neurons. However, it is not known if these differences are only expressed during the course of development. We will not consider functional differences other than the receptor distribution described in the Connectivity section between CA3 Pyramidal Cells and CA3 Neurons (Associational Pathway).

CA1 PYRAMIDAL CELL TO CA1 NEURONS CONNECTIVITY (ASSOCIATIONAL PATHWAY)

Phaseolus vulgaris leucoagglutin injections in CA1 area showed clear gradients of projection in both the septotemporal and transverse axis (Amaral et al., 1991). CA1 pyramidal cells located in the mid part along the septotemporal axis are characterized by the following properties: 1) Proximal CA1 pyramidal cells (i.e., at the border of the CA2 region) project to the distal parts of the subiculum and collateral branches extend throughout the whole extent of CA1 area in stratum oriens. 2) CA1 pyramidal cells located in the mid part along the transverse axis are characterized by a small circular area of associational connectivity in stratum oriens (200 μm radius) and a further projection toward the subiculum with collateral branching as described for proximal CA1 pyramidal cells. 3) Distal CA1 pyramidal cells project to nearby areas in the subiculum with some fibres backtracking to the CA1 area at the border of stratum radiatum and moleculare. They do not appear to extend further backward than their locus of origin. Intracellular labeling of CA1 pyramidal cells showed that very few collaterals enter the stratum radiatum (Tamamaki and Nojyo, 1990). Evidence for a CA1 associational pathway has been gained indirectly (Christian and Dudek, 1988) and directly (Thomson

and Radpour, 1991) using electrophysiological techniques. In the slice, the probability of connection between CA1 pyramidal cells is very low, around 1/130, and the postsynaptic response is characterized by an important NMDA receptor-mediated component. The peak amplitude of the NMDA component is 0.23 mV and the non-NMDA one is 0.13 mV (Thomson and Radpour, 1991). The failure of transmission is thought to be around 20%. According to the spatial gradients of connectivity (Amaral et al., 1991), we would expect a higher probability for cells located in the mid part and an even higher value for the cells which project backward.

Electrophysiological recordings show the existence of synaptic contacts with interneurons (Knowles and Schwartzkroin, 1981; Lacaille et al., 1987). The probability of a pyramidal-basket cell connection in the longitudinal slice is 0.3 (Knowles and Schwartzkroin, 1981). The probability of the polysynaptic pathway pyramidal cell-interneuron-pyramidal cell is 0.13. The probability of a pyramidal-O/A cell connection in the transverse slice is 0.64, the average EPSP amplitude is 2.2 mV, and the probability of transmission is 0.64 (Lacaille et al., 1987). No connections were found between CA1 pyramidal cells and L-M interneurons (Lacaille and Schwartzkroin, 1988b). However, such connections may exist (Lacaille, personal communication) and so we have given them a low probability.

It is interesting to note that in both CA3 and CA1 associational pathways, the probability of connection is considerably biased toward that of the interneurons. Thus the primary function of these pathways may be in inhibitory feedback control.

CA1 INTERNEURONS

Fortunately, considerable more information is available about inhibitory interneurons in the CA1 area. They inhibit pyramidal cells through the activation of $GABA_A$(Traub et al., 1987a) and $GABA_A$ (Alger and Nicoll, 1982b; Alger, 1984; Segal, 1990a; Williams and Lacaille, 1992) receptor-mediated IPSPs (Alger and Nicoll, 1980; Collingridge et al., 1984). Two types of interneurons have been distinguished electrophysiologically (Kawaguchi and Hama, 1987, 1988). Fast spiking cells contain parvalbumin (Kawaguchi et al., 1987) and provide feedforward and feedback inhibition, whilst non-fast spiking cells (L-M interneurons) are thought to provide feedforward inhibition only. To date, four distinct types of interneurons have been identified: chandelier cells (Somogyi et al., 1983, 1985; Li et al., 1992) and basket cells (Schwartzkroin and Mathers, 1978; Schwartzkroin and Prince, 1980; Ashwood et al., 1984; Schwartzkroin and Kunkel, 1985; Kawaguchi and Hama, 1987, 1988), which are both located near the stratum pyramidale, Oriens/Alveus (O/A) interneurons (Lacaille et al., 1987; Lacaille and Williams, 1990), which are located in the stratum oriens near the alveus, and lacunosum-moleculare (L-M) interneurons (Kawaguchi and Hama, 1987, 1988; Lacaille and Schwartzkroin, 1988a,b; Fraser and MacVicar, 1991; Williams and Lacaille, 1992). Since interneurons in area CA1 contact each other (Lacaille et al., 1987; Kunkel et al., 1988), we have assumed that basket cells and O/A interneurons reciprocally inhibit each other and that L-M interneurons inhibit basket cells and O/A interneurons. We have also assumed the presence of recurrent collaterals.

CA1 chandelier cells

In a completely HRP-filled chandelier cell in area CA1 three dendrites can be distinguished in the stratum radiatum with a 200 μm transverse extension (Li et al., 1992). In stratum oriens the extension is 300 μm. The axonal arborization is contained in an ellipse with the principle axis 0.85 mm along the longitudinal direction and the small axis 0.6 mm along the transverse direction. From the figures listed in Appendix A1 there are 9,424 pyramidal cells in this elipse which results in a probability of connection between one chandelier cell and a given pyramidal cell of 0.13. In contrast to other computer models (Douglas and Martin, 1990; Lytton and Sejnowski, 1991) we propose that their role is also to block all eventual spike activity in the postsynaptic cell during a certain time window. Since it is not known if this strict control of pyramidal cell activity extends to the other interneurons in CA1 area we have assumed that chandelier cells contact basket cells. Since axo-axonic CA3 neurons seem to generate IPSPs in CA3 pyramidal cells we have adopted the same property for CA1 chandelier cells.

CA1 basket cells

Very few anatomical data are available about basket cells. Fifteen dendritic branches can be found in the stratum radiatum covering a distance of 120 μm on the transverse direction and ten branches in the stratum oriens covering a distance of 150 μm (Kawaguchi and Hama, 1987). The axonal arborization covers a wide area, at least in the transverse direction (Schwartzkroin and Kunkel, 1985; Kawaguchi and Hama, 1988). Since paired recordings (basket-pyramidal cells) in the longitudinal direction (Knowles and Schwartzkroin, 1981) do not mention the distance between the linked cells we have assumed a 0.8 mm extension in the longitudinal direction. As a first approximation we have taken a connectivity pattern similar to the one described for chandelier cells, i.e., an elliptical field. In longitudinal slices the probability of basket–pyramidal cell connection is 0.3 (Knowles and Schwartzkroin, 1981). Basket cells contact other interneurons (Misgeld and Frotscher, 1986; Nitsch et al., 1990). Since fast and slow IPSPs can be recorded in basket cells following activation of Schaffer/commissural pathway (Lacaille, 1991) it is likely that they also receive contacts from all other interneurons. However, the direct activation of GABAergic fibres (like septum fibres) cannot be excluded (Freund and Antal, 1988). In a 400 μm thick slice there are 243 parvalbumin-reactive neurons (Best et al., 1993a) of which 203 are parvalbumin-immunoreactive basket cells and the remaining 40 are chandelier cells (Best et al., 1993a,b). In this area all parvalbumin-reactive neurons are also GAD immunoreactive, and thus as a first approximation we have not taken into consideration parvalbumin-negative basket cells (Kosaka et al., 1987; DeFelipe et al., 1989; Nitsch et al., 1990; Soriano et al., 1990).

CA1 O/A interneurons

We consider as belonging to the same population the O/A interneurons proper (Lacaille et al., 1987) and the so-called vertical cells (Lacaille and Williams, 1990). Their dendrites extend into all strata (Lacaille and Williams, 1990). The axonal arborization seems to cover a wide area in the transverse direction,

projecting onto basal dendrites and soma of pyramidal cells and other interneurons (Lacaille et al., 1987). We have assumed that the dendritic arborization can also be represented by an elliptical field. In transverse slices the probability of O/A-pyramidal cell connection is 0.07 (Lacaille et al., 1987). The IPSP amplitude is 2.0 mV in average (Lacaille et al., 1987) and seems to be mediated by $GABA_A$ receptors only (Madison and Nicoll, 1988; Samulack and Lacaille, 1991). However, a recent study suggests the existence of two populations of O/A interneurons. The first of these receives recurrent excitation from CA1 pyramidal cells and produces $GABA_A$ receptor-mediated inhibition. The second does not receive this recurrent excitation and produces either a mixture of $GABA_A$ (75%) and $GABA_B$ (25%) receptor-mediated inhibition or $GABA_B$ receptor-mediated inhibition only (Samulack et al., 1993). The same study suggests that synapses of the first population on CA1 pyramidal dendrites are electrotonically more distant from the soma than those of basket cells (Samulack and Lacaille, 1993).

CA1 L-M interneurons

L-M interneurons have been described as non-fast spiking cells (Kawaguchi and Hama, 1987) with membrane properties very different from those of pyramidal cells (Williams and Lacaille, 1993). Dendrites extend in the stratum lacunosum-moleculare, radiatum, and oriens and have a very wide extension in the transverse slice (Lacaille and Schwartzkroin, 1988a). The axonal arborization seems to cover a wide area in both transverse and longitudinal directions, projecting in stratum pyramidale and sometimes in the stratum oriens (Lacaille and Schwartzkroin, 1988a). We have assumed that the axonal arborization can also be represented by an elliptical field with the long axis parallel to the longitudinal one. We have taken a longitudinal extension of 1.0 mm (Lacaille and Schwartzkroin, 1988a). In transverse slices the probability of L-M-pyramidal cell connection on pyramidal cell is 0.64 and the average IPSP amplitude is 0.91 mV in the soma and 0.67 mV in the dendrites (Lacaille and Schwartzkroin, 1988b). However, this IPSP is only produced when L-M interneurons are bursting (Lacaille and Schwartzkroin, 1988b) and seems to be mediated by the activation of $GABA_B$ receptors (Williams and Lacaille, 1992). The probability of L-M-basket cell connection is 0.5 and the IPSP amplitude is 0.91 mV (Lacaille and Schwartzkroin, 1988b). Two functional types of interneurons can be distinguished: One hyperpolarizes the dendritic membrane of pyramidal cells and the other one shunts it (Alger and Nicoll, 1982a). Stimulation of afferents in stratum radiatum produces a complex response which is the result of the activation of NMDA, non-NMDA, and $GABA_A$ receptors (Lacaille et al., 1993). The activity of L-M interneurons is thus also controlled by feedforward inhibition. We assume that it is due to the activation of O/A interneurons and basket cells. Finally, it will be noted that L-M interneurons are characterized by low-threshold transient calcium currents (Fraser and MacVicar, 1991).

CONNECTIVITY MODEL OF THE HIPPOCAMPUS

In this section we describe the various connectivity patterns in CA1 and CA3 for the different classes of cells found in our model. In particular, we will identify the number and location of the different synapses and their dependence on the values of the different parameters. As stated previously the software constructs files containing the spatial location of the different synapses, their probability of activation, the receptors involved, and their synaptic weights.

Schaffer/commissural-CA1 neurons pathway

We first modeled the whole extent of CA3 and CA1 areas. In this model we used 193,600 CA3 pyramidal cells, which were distributed as follows: 121 along the transverse axis, 400 along the longitudinal axis, and four deep in the pyramidal cell layer. The 318,600 CA1 pyramidal cells were distributed as follows: 118 along the transverse axis, 540 along the longitudinal axis, and five deep in the pyramidal cell layer (see Appendix A1).

In the following CA1 neurones are characterised by their co-ordinates (X,Y) along the transverse and longitudinal axis respectively. X represents the abscissae of the neuron along the transverse axis, where X = 0 corresponds to the most proximal cell. Y is the conterpart the longitudinal axis, where Y = 0 corresponds to the cell located at the temporal end (Fig. 1d). (x,y) are used for CA3 neurones.

According to anatomical data (Ishizuka et al., 1990) we assume that each CA3 pyramidal cell is characterized by the same gross features of connectivity pattern (see Fig. 2a): 1) an area where the probability of connection is the highest, the position of which depends upon the transverse location of the emitting CA3 pyramidal cell, and 2) a probability of connection with cells outside this area which decreases with distance. We have adopted the following model (see Fig. 3): For each CA3 pyramidal cell we first computed the point (X_{max}, Y_{max}) where the density of connection is the highest. Two axes were then determined: one had a septal-proximal CA1/temporal-distal CA1 orientation (I axis) and its perpendicular (J axis). The intersecting point was (X_{max}, Y_{max}). These two axes reflect the pattern of density of distributions found experimentally (Ishizuka et al., 1990). Each point along the I axis was given a probability of innervation by an axonal branch of a CA3 pyramidal cell. This probability decreased with the distance from X_{max}. Since the probability of connection seems to be high even some distance away from X_{max}, we assumed a Gaussian distribution with wide dispersion along the I axis. At X_{max} the probability is 1.0. Along the J axis the distribution of probability is also Gaussian with smaller dispersion since the probability drops quickly with distance from Y_{max} along the J axis. At Y_{max} the probability is also 1.0. The probability of there being a connection of (X_{max}, Y_{max}) is thus $1.0 \times 1.0 = 1.0$. We assume as a first approximation that the two Gaussian distributions are the same for all CA3 pyramidal cells, and that the angle between I and transverse axis is 45° as obtained from our own measurements of Ishizuka's data (Ishizuka et al., 1990). For proximal CA3 pyramidal cells (x = 0, y = 200, for example), the area of maximum density is located septally in distal CA1 ($X_{max} = 117, Y_{max} = 270$), and for distal CA3 pyramidal cells (x = 120,y = 200 for example) the area of maximum density is located temporally in proximal CA1 ($X_{max} = 0, Y_{max} = 270$).

On Figure 4 we simulated a *P. vulgaris* leucoagglutin injection experiment in CA3. Three circular areas (100 μM radius) located in the mid part along the longitudinal axis and in

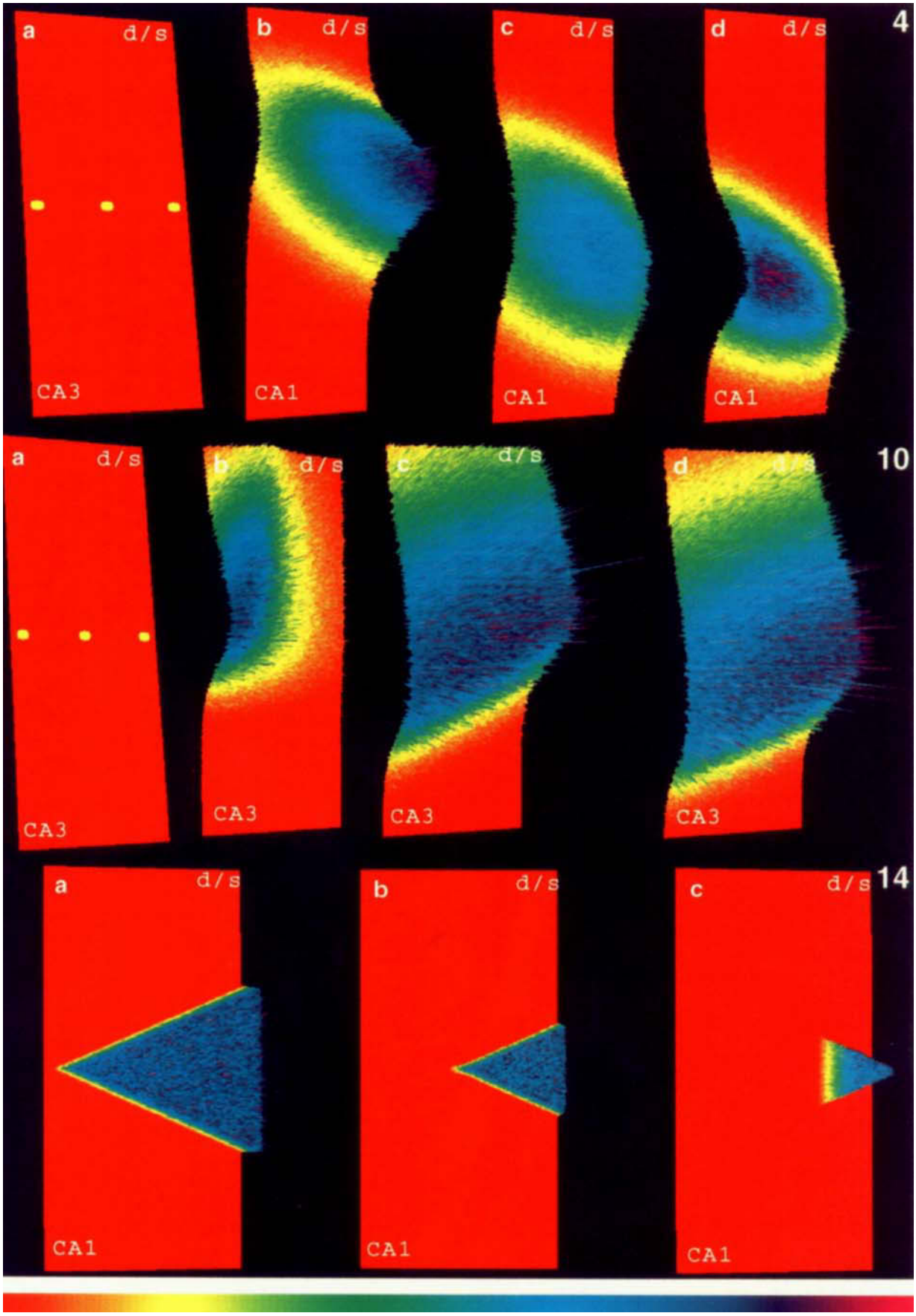

Figs. 4, 10, and 14.

proximal, mid, and distal CA3 along the transverse axis, respectively, were "labeled" (Fig. 4a). The number of synapses that the labeled CA3 pyramidal cells located inside each area made with CA1 pyramidal cells was then computed. Proximal CA3 pyramidal cells projected heavily septally in distal CA1 (Fig. 4b), mid CA3 pyramidal cells had a more diffuse area of projection in mid CA1 (Fig. 4c), and distal CA3 pyramidal cells projected heavily temporally in proximal CA1 (Fig. 4d). These results appeared to be in good agreement with previous anatomical data (Ishizuka et al., 1990). Given these spatial gradients of connectivity we investigated the relationship between the number of synapses and the location of the emitting and receiving neurons.

We first sampled the CA1 pyramidal cells located in the mid part of CA1 along the longitudinal axis and on the surface of the pyramidal cell layer (Y = 270) for all these cells). On this occasion 118 CA1 pyramidal cells were counted along the transverse axis. The neuron whose abscissae is X = 0 corresponds to the most proximal CA1 pyramidal cell, and the neuron whose abscissae is X = 117 corresponds to the most distal one (see Fig. 1d). Figure 5a shows the number of synapses made by all emitting CA3 pyramidal cells as a function of the abscissae of the receiving CA1 pyramidal cell along the transverse axis. The modeling suggests that there is a gradient in the number of synapses a given CA1 pyramidal cell receives from all CA3 pyramidal neurons: Proximal and distal neurons receive fewer synapses (6,500) than those located in the mid region (8,000). Assuming five synaptic contacts per fibre, we obtain a range of 32,500–40,000 synapses, a figure comparable to that recently reported (Li et al., 1993). If we assume that commissural fibres follow the same connectivity rule the total number of connections from both contralateral and ipsilateral CA3 areas is $2 \times 8{,}000 = 16{,}000$ for mid CA1 pyramidal cells. Since we do not yet know the branching pattern of Schaffer collaterals we decided to represent their connectivity pattern by a matrix of probability for a given axonal branch to cross the dendritic tree of a given CA1 pyramidal cell. Let us hypothesize that an axonal branch crosses a given CA1 pyramidal cell dendritic tree if the corresponding probability element in the matrix is higher than 0.1. In this case, 115,000 axonal branches cross the dendritic tree of a mid CA1 pyramidal cells (Fig. 5b). In the whole hippocampus the connectivity (i.e., the ratio between the number of existing connections and the number of possible connections) is thus $8{,}000/115{,}000 = 0.07$. Conversely, we looked at a string of CA3 pyramidal cells located in the mid part of CA3 along the longitudinal axis (y = 200 for all these cells). One hundred twenty-one neurons were counted along the transverse axis. Again x = 0 (x = 120) corresponded to the most proximal (distal) cell. Mid CA3 pyramidal cells made more synaptic contacts with CA1 pyramidal cells than those from the proximal and distal regions (Fig. 5c), 13,000 synapses for mid CA3 neurons compared with 11,000 for proximal or distal ones. Since most experimentalists and modelers are interested in phenomena occurring in the slice we applied the previous analysis to a 400 μm thick slice. We kept the same connectivity matrix and "cut" the slice in the mid part of the hippocampus. The distribution of the number of synapses is given in Figure 5d. The number of CA3 cells which make direct contact with CA1 pyramidal cells is considerably reduced, 580 on mid CA1 pyramidal cells compared with 8,000 for the whole structure. However, the ratio between the two previous values (13.8) does not mirror the ratio between the thickness of the slice and the length of the hippocampus (20.0). This discrepancy is explained by the fact that projection is constrained in a solid angle which contains the thickness of the slice. Even if many fibres are cut in the slice, either at its septal or temporal border, the number of synapses is higher in proportion to that found in the whole structure. If a uniform distribution is used to describe the projection from CA3 to CA1, the ratio would be 20.0. The probability of finding a CA3 pyramidal cell-CA1 pyramidal cell connection

Fig. 4. Simulation of a *Phaseolus vulgaris* leucoagglutin labeling experiment. **a:** CA3 area; **b–d,** CA1 area. a: Unfolded CA3 area as in Figure 2 contains 193,600 pyramidal cells as described in the main text (see Connectivity Model of the Hippocampus in text). CA1 has 318,600 CA1 pyramidal cells. The parameters (see Appendix B) are G31_1 = 9, G31_2 = 90, G31_3 = 65, and p31 = .06. In all three cases (b–d) the projecting cells are at middle septotemporal level as suggested in a. b: Pattern of projection from proximal CA3 pyramidal cells (circle of 100 μm radius centred on cell the coordinates of which are x = 10, y = 200 along the transverse and the longitudinal axes, respectively). c: Pattern of projection from mid CA3 (centred on cell the coordinates of which are x = 60, y = 200). d: Pattern of projection from distal CA3 (centred on cell the coordinates of which are x = 110, y = 200). It is clear from these figures that proximal CA3 pyramidal cells project massively septally in distal CA1, mid CA3 pyramidal cells project in mid CA1, and distal CA3 pyramidal cells project temporally in proximal CA1. The scale of bar indicates the number of connections, from 0 (red) to 100 (purple). As in Figures 10 and 14, d/s represents the distal and septal part of each CA3 and CA1 areas of the hippocampus. For the sake of clarity CA3 and CA1 areas have been separated.

Fig. 10. CA3 associational pathway. The same cells as in Figure 4 were "labeled" **a** and their corresponding associational projection areas in CA3 are shown on b–d. The set of parameters was G33_1 = 90, G33_2 = 40, G33_31 = 10, G33_32 = 200, and p33 = .03. **b:** Proximal cells project locally along the transverse axis and extensively in the longitudinal direction with a preferential septal orientation. **c:** Cells located in the mid part have a distal-septal to proximal-temporal orientation. **d:** Distal cells have the similar projection, displaced temporally. Scale bar same as as for Figure 4.

Fig. 14. Simulation of a *P. vulgaris* leucoagglutin labeling experiment in the CA1 area. The unfolded CA1 area contains 318,600 CA1 pyramidal cells. The parameters are G11 = 4, p11_0 = .01, p11_10 = .02, p11_11 = .01, and p11_2 = .01. **a:** Projection from proximal CA1 pyramidal cells (circle of 100 μm radius centred on cell the co-ordinates of which are X = 10, Y = 270 along the transverse and the longitudinal axes, respectively). **b:** Projection from mid CA1 (centred on cell the coordinates of which are X = 59, Y = 270). c. Projection from distal CA3 (centred on cell the co-ordinates of which are X = 110, Y = 270). The projection is uniform in the triangle defined by the dispersion angle. There is a very faint small local circular pattern of connections around the cells located in the mid part of CA1 in b. Red represents 0 and purple represents 5 synapses.

in the slice is 580/9,680 = .06 (9,680 = 121 × 20 × 4 represents the number of CA3 pyramidal cells in the slice). This probability is higher than that found in the whole structure, i.e., 8,000/193,600 = .04. Interestingly, the shape of the curve of the distribution of synapses is different. There are, in proportion, more synapses from CA3 pyramidal cells on proximal CA1 cells in the slice than in the whole structure, whereas the probability of finding a connection between a CA3 pyramidal cell and a distal CA1 pyramidal cell drops dramatically (compare Fig. 5a and d).

These results show that 1) the first three-quarters of the CA1 pyramidal cells receive the vast majority of the ongoing activity in the slice and 2) slicing perpendicularly to the longitudinal axis is sufficient if one is to attempt paired CA3-CA1 pyramidal cell recordings. We suggest that a high probability of obtaining paired recordings is gained by placing the recording electrode in the proximal part of CA1 and the other electrode in distal CA3, deep in the slice. We obtained the last result after displaying the CA3 cells that were connected to a given proximal CA1 cell (data not shown). Cutting at various angles might increase the difficulty of finding such paired connections. However, the highest probability was obtained by cutting the slice with a temporal orientation of −22° which corresponds to the angle of maximum density projection for distal CA3 pyramidal cells and by recording in most distal CA3 and most proximal CA1 regions. One should bear in mind that distal CA3 pyramidal cells do not give rise to Schaffer collaterals proper and that they project to the stratum oriens of CA1.

We then tried to characterize possible functional groups, i.e., groups of CA1 pyramidal cells, that share common afferents. This issue is fundamentally important if one is to understand the dynamics and functioning modes of the system. We selected three CA1 pyramidal cells in the mid part of the hippocampus (with respect to the longitudinal axis, Y = 270) located on the proximal, mid, and distal part of a transverse string, respectively. The proximal cell (X = 5) receives 6,664 synapses from the whole CA3 pyramidal cell population. We then counted the number of shared inputs by all its neighbours (Y = 270 for all these cells) along the transverse string (Fig. 6a). It appears that this cell shares more inputs with cells located near the mid part of the string (550, i.e., 8%) than with its nearest neighbours (460, 7%). As one expects it shares fewer inputs with distal cells (400, 6%). The mid cell (X = 58) receives 7,986 synapses from the whole CA3 pyramidal cell population and shares the maximum inputs with its close neighbours (720, 9%). This number decreases with the distance dropping to 510 (6%) for proximal and distal cells (Fig. 6b). The distal cell (X = 115) receives 6,585 synapses from the whole CA3 pyramidal cell population and shares its inputs preferentially with close neighbours and cells located toward the mid part of the slice (550, 8%). Conversely it shares less inputs with proximal cells (390, 6%; Fig. 6d). Two main features can thus be established. First, a given CA1 pyramidal cell in the whole hippocampal structure shares few inputs originating from the whole CA3 pyramidal cell population with its neighbours (around 8%), supporting a wide divergence of activity. Second, inputs are preferentially shared with cells located in the mid part along the transverse axis rather than with distal and proximal cells. We repeated these simulations for the same three CA1 pyramidal cells counting this time the number of inputs in the slice. The proximal cell is connected to 573 CA3 pyramidal cells in the slice. On this occasion, the pattern of shared inputs is totally different (Fig. 6d). Inputs are

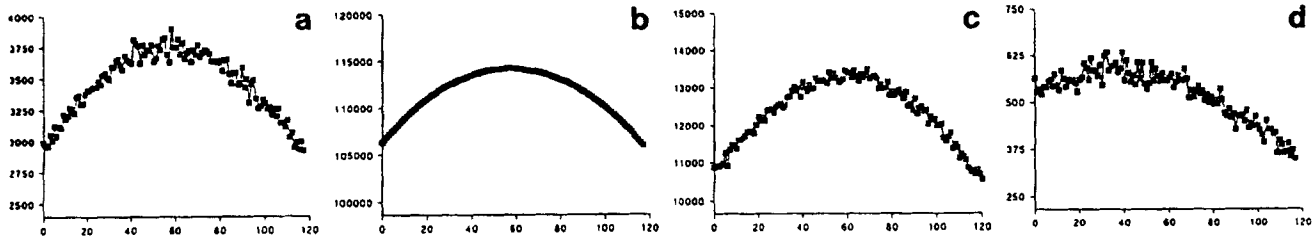

Fig. 5. In this and all similar figures the numbers on the abscissae represent the cell co-ordinate along the transverse axis, i.e., x for CA3 cells and X for CA1 cells. The ordinate represents the number of synapses made on those cells. The single spots in these graphs are interconnected with lines to increase visibility and to allow easier extraction of data from the graphs. They do not correspond to continuous processes; they are single observations. Finally, the scale of the ordinate is different for each graph. We found this representation to be more informative since adopting a common scale (i.e., 0–120,000 for **b**) would have transformed the curve in d into a straight line. The fine details of the projection and/or the statistical fluctuations would have thus been missed. **a:** Convergence from CA3 to CA1. This graph shows the evolution of the number of pyramidal cells in the whole CA3 area contacting a given CA1 pyramidal cell in the mid septotemporal part of the hippocampus as a function of the transverse location of the receiving CA1 pyramidal cell (Y = 270 for all these cells). The bell shape of the curve indicates that mid CA1 pyramidal cells receive more inputs than proximal and distal neurons. **b:** Number of Schaffer collateral branches (see text) crossing each of the previous CA1 pyramidal cells. The bell shape mirrors the previous one. **c:** Divergence from CA3 to CA1. This graph shows the evolution of the number of CA1 pyramidal cells a given CA3 pyramidal cell is contacting as a function of the transverse location of the emitting CA3 pyramidal cell (y = 200 for all these CA3 pyramidal cells). The number of connections in c is higher (greater divergence) than in a since CA1 pyramidal cells are more numerous than CA1 ones. However, the same general feature is kept, i.e., mid CA3 cells contact more neurons than proximal and distal ones. **d:** Same as a but in a slice. Note the difference between the two curves: Mid CA1 pyramidal cells still receive more connections but there is a great discrepancy between the connectivity patterns of distal and proximal neurons (see text). For all the above, the simulation parameters were G31_1 = 9, G31_2 = 90, G31_3 = 65, and p31 = .06.

shared locally with the nearest neighbors (75, 13%) and decrease with the distance (40, 7% for the most distal cells). The same general features apply to the mid cell (Fig. 6e) which receives 582 inputs that are preferentially shared locally (75, 13%). The number of shared inputs decreases distally (35, 6%) but stays high proximally (60, 10%). The distal cell receives 384 inputs and shares more of these with proximal and mid cells (50, 13%) than with distal ones (30, 8%; Fig. 6f). As a consequence, if the activity carried along the Schaffer collateral pathway appears more spread out in the whole structure, it seems much more structurated locally, in the thickness of the slice. In such a narrow band, CA1 pyramidal cells tend to share their inputs with cells located in the mid and proximal part of the transverse axis.

All the fore mentioned values were obtained with a fixed set of parameters (G31_1 = 9, G31_2 = 90, G31_3 = 65, and p31 = .13). We then performed a parametric study in order to test the robustness of the results to modifications in the values of parameters. G31_1 controls the dispersion of the distribution which gives the spatial orientation of the Schaffer collaterals. Even considerable variation of this parameter does not change the general features of the results (data not shown). More interesting are G31_2 and G31_3, which control the dispersion of the Gaussian distributions involved in building the probability matrix (see Fig. 3). We first varied G31_2 which controls the distribution along the I axis. Small values indicate a narrow dispersion (i.e., a highly peaked distribution) and high values indicate a wide dispersion, i.e., the probability of finding a connection is high even some distance away from X_{max} along the I axis. To illustrate the changes brought about by the variations in G31_2 we plotted the number of CA3 pyramidal cell–CA1 pyramidal cell connections in the slice as a function of the location of the CA1 pyramidal cells (Y = 270) along the transverse axis (see Fig. 6d). The different shapes obtained for various values of G31_2 are shown on Figure 7. Apart from slight variation in the number of connections the general features are not changed. This is not surprising since the dispersion varies between values which remain quite large and thus do not influence the pattern of distribution along the transverse axis. We repeated the simulations varying G31_3 (Fig. 8). The shape of the curve and the number of synapses are dependent upon the values of the parameter. A narrow dispersion gives fewer connections (120–430) and a greater discrepancy between proximal and distal cells than a wide dispersion (475–650, compare Fig. 8a and f). Modifications of the distribution along the J axis have thus important consequences since the domain of variation of the parameter considerably changes the characteristics of the dispersion (from very narrow to wide). The probability of connections varies accordingly, from 0.04 (G31_3 = 30) to 0.07 (G31_3 = 100) without changing the general features. Finally, we fixed G31_2 and G31_3 and varied p31 which directly controls the probability of connections. The number of connections is a straightforward function of p31 as can be seen on Figure 9. Low values of p31 give fewer connections, hence a lower probability of connection (0.025 for p31 = 0.06). Greater values of p31 give a higher probability (0.098 for p31 = 0.20). The general features are the same: Preferential connections are found in mid CA1, and the probability decreases slowly toward the proximal end and rapidly toward the distal one.

This parametric study shows that the general results are fairly robust against changes in the values of the parameters. Thus, within the constraints of this model, the results described above appear to be general properties of the system.

The projection pattern from CA3 pyramidal cells to CA1 interneurons has the same general features since interneurons

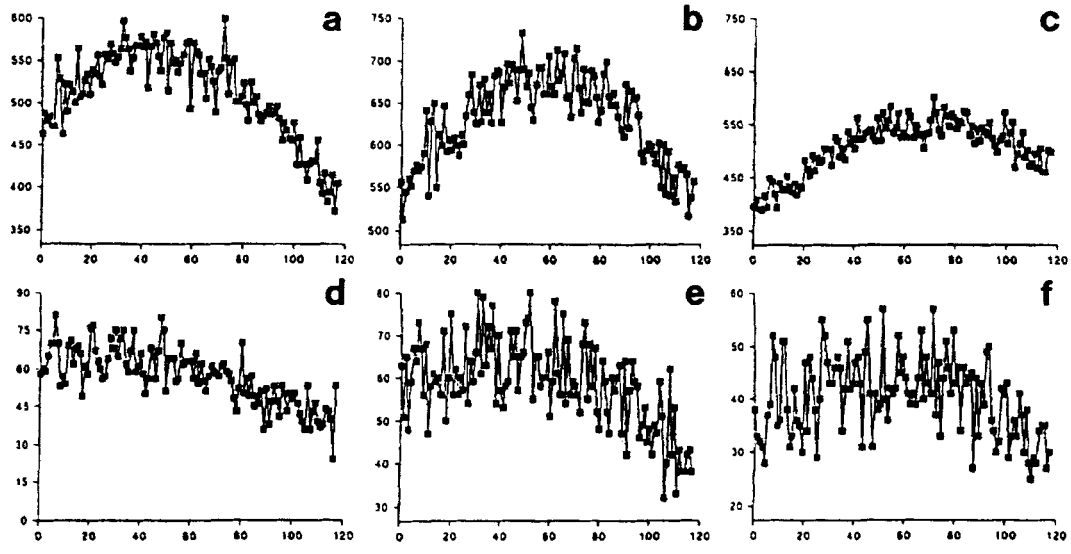

Fig. 6. Number of shared inputs along the transverse axis for a proximal **(a)** mid **(b)**, and distal CA1 cell **(c)** in the whole hippocampus. In a, X = 5. The cell is sharing more inputs with mid cells than with its nearest neighbors and much less with distal cells. In b, X = 58. This cell shares more inputs with its neighbours and less with proximal and distal ones. In c, X = 115. The shape is a mirror image of that in a, i.e., the cell shares more inputs with cells located toward the mid part (distal side) and few with proximal ones. **d–f:** as a–c, but in a slice. The patterns are totally different. Discrepancies between distal and proximal ends are much less marked and the proportion of shared inputs is higher. The parameters were G31_1 = 9, G31_2 = 90, G31_3 = 65, and p31 = 0.06.

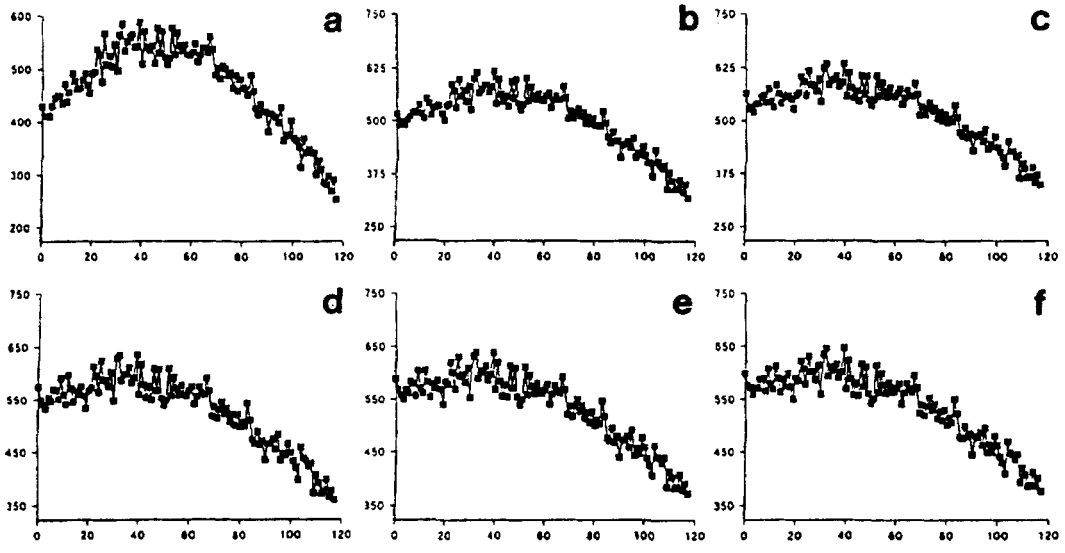

Fig. 7. Variation of the number of connections (as in Fig. 5a) as a function of G31_2. **a:** G31_2 = 45. **b:** G31_2 = 65. **c:** G31_2 = 85. **d:** G31_2 = 95. **e:** G31_2 = 115. **f:** G31_2 = 135. All other parameters are unchanged. Variations in G31_2 do not change the general characteristics of the pattern of projection.

can be seen, from the model point of view, as pyramidal cells spread out with a lower density.

CA3 Associational pathway

We will consider the whole extent of CA3 area which contains 193,600 pyramidal cells and a 400 μm thick slice which contains 9,680 neurons (see Appendix A). As in the previous section the connectivity pattern is characterized by the following features: first, an area with maximal density of projections centered on point (x_{max}, y_{max}) the locus of which depends upon the transverse location of the emitting CA3 neuron (septally for proximal cells and temporally for distal ones) and second, a matrix of probability of connection oriented along two axes I and J as derived from experimental data (Ishizuka et al. 1990). Here, the orientation of I axis, i.e., its angle in relation to the transverse axis, depends upon the transverse location of the CA3 neuron. The Gaussian distribution of probability depends upon two parameters, G33_1 and G33_2, which control the dispersion toward the septal and temporal ends, respectively. The distribution of probability along J axis depends upon the transverse location of the cell. The parameter con-

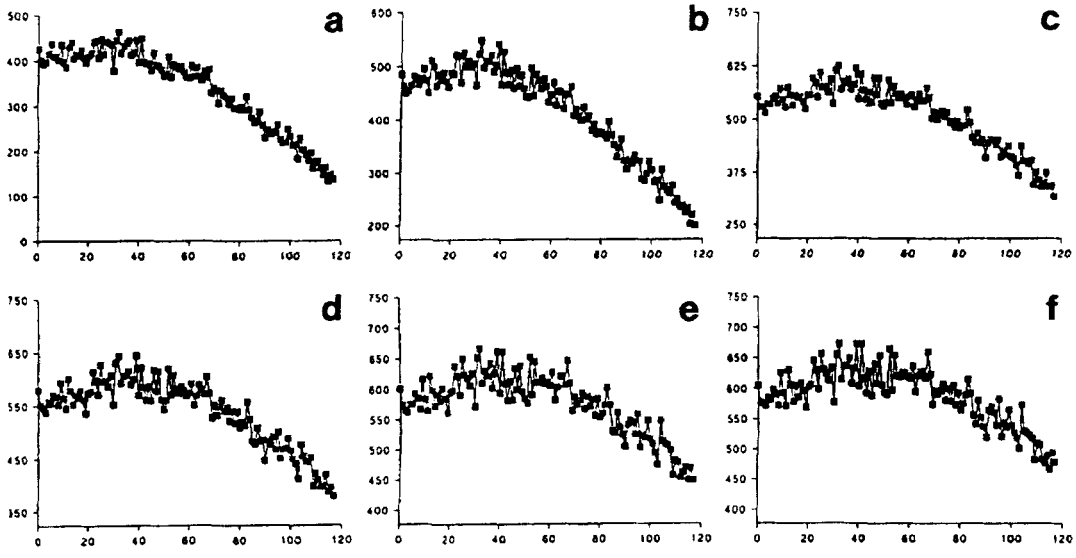

Fig. 8. As Figure 7 for a variation of G31_3. **a:** G31_3 = 30. **b:** G31_3 = 40. **c:** G31_3 = 60. **d:** G31_3 = 70. **e:** G31_3 = 90. **f:** G31_3 = 100. All other parameters are unchanged. Variations in G31_3 do not change the general characteristics of the pattern except the number of connections.

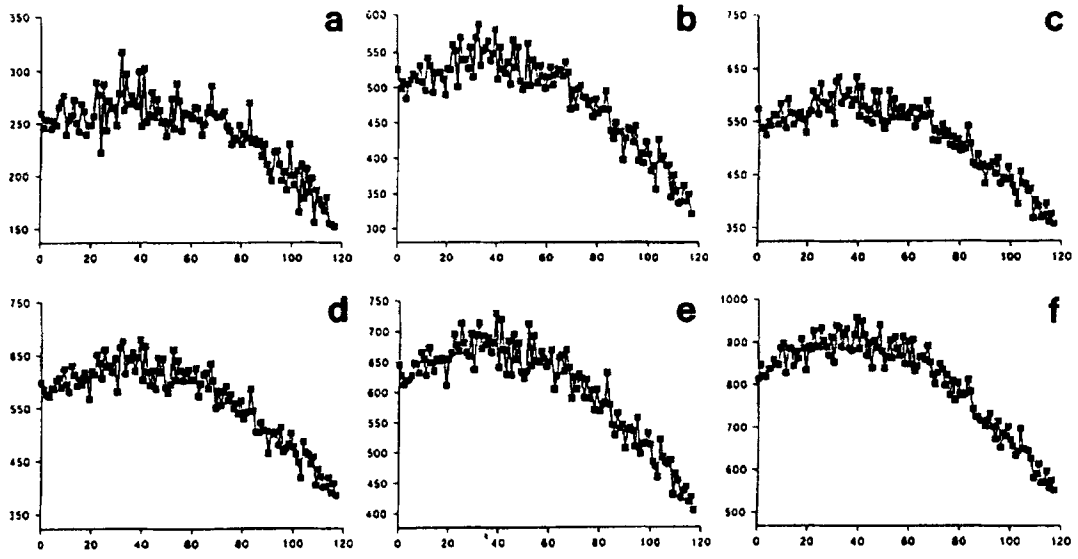

Fig. 9. As Figure 7 for a variation of p31. **a:** p31 = .06. **b:** p31 = .12. **c:** p31 = .13. **d:** p31 = .14. **e:** p31 = .15. **f:** p31 = .20. All other parameters are the same. Again the general features are not modified except that the number of connections is strongly dependent upon the value of p31.

trolling the dispersion G33_3 varies between G33_31 and G33_32. G33_31 has a small value as the dispersion is very narrow and G33_32 has a high value as the dispersion is very wide (see Fig. 3). The variation between G33_31 and G33_32 is not linear as it is clear from Figure 3 that the dispersion becomes wide very quickly when reaching the mid part of CA3 and that it does not change much more distally. The variation of G33_3 follows a highly peaked Gaussian distribution which gives a very low value for G33_3 for the most proximal cells and high values for the others. Simulations were performed with the following set of parameters: G33_1 = 90, G33_2 = 40,G33_31 = 10, G33_32 = 200, and p33 = .03.

Figure 10 shows a simulation of a *P. vulgaris* leucoagglutin injection experiment. Three circular areas (100 μM radius) located in the mid part along the longitudinal axis and in proximal, mid, and distal CA3 along the transverse axis, respectively, were "labeled" (Fig. 10a). The number of synapses the labeled CA3 pyramidal cells made on CA3 pyramidal cells was then computed. Proximal CA3 pyramidal cells project locally in the transverse direction and heavily septally (Fig. 10b), mid CA3 pyramidal cells have a more diffuse area of projection centred somewhat more proximally in CA3 (Fig. 10c), and distal CA3 pyramidal cells project even more diffusely mainly in temporal and proximal directions (Fig. 10d). These results, which are in good agreement with anatomical data (Ishizuka et al., 1990), clearly indicate that local groups of cells play very different roles in the distribution of their activity to other cells according to their transverse location.

As in the previous section, we investigated for the whole structure the number of associational connections as a function of the transverse location of the receiving CA3 pyramidal

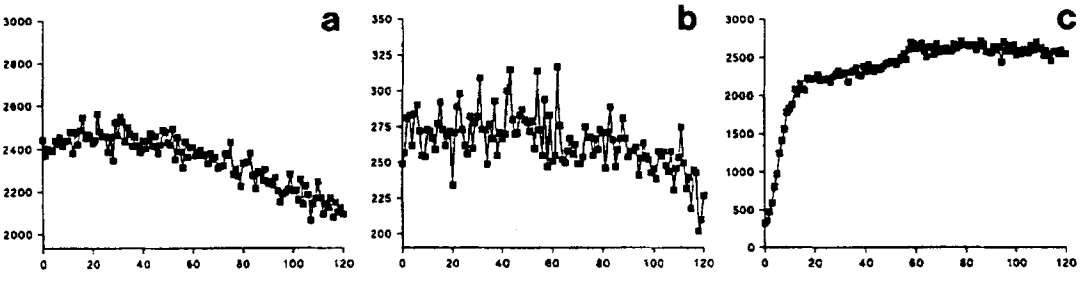

Fig. 11. **a:** Convergence from CA3 to CA3. This graph shows the evolution of the number of pyramidal cells in the whole CA3 area contacting a given CA3 pyramidal cell in the mid septotemporal part of the hippocampus as a function of the transverse location of the receiving CA3 pyramidal cell (y = 200 for all these cells). The convergence decreases toward the distal end of the CA3 area. **b:** Same as a but for a slice. Note that the connectivity pattern is unchanged. **c:** Divergence from CA3 to CA3. This graph shows the evolution of the number of CA3 pyramidal cells a given CA3 pyramidal cell is contacting as a function of the transverse location of the emitting CA3 pyramidal cell (y = 200 for all these cells). Proximal cells have very few associational connections. This number increases toward the middle of the proximo-distal distance and thence stays constant. The set of parameters was G33_1 = 90, G33_2 = 40, G33_31 = 10, G33_32 = 200, and p33 = .03.

cells located in the mid part of the longitudinal axis (y = 200; Fig. 11a). The number of connections varies between 2,500 for the most proximal cells and 2,100 for the most distal ones. The corresponding probabilities of connection in the whole structure are thus 2,500/193,600 = .013 and 2,100/193,600 = .011. As one would expect from the connectivity rules, proximal cells receive the majority of inputs as all cells project toward proximal CA3. We then performed the same analysis in the slice (Fig. 11b). As in the whole structure, we obtain a higher density of connections in proximal CA3. The corresponding probabilities are 300/9,680 = .031 and 210/9,690 = .022. Again the ratio between the number of connections, 2,500/300 = 7.0, does not mirror the ratio between the length of the whole structure and the thickness of the slice, which is 20.0. This is due to the fact that the connections are local and do not extend to far in the longitudinal direction. The probability of finding direct CA3–CA3 pyramidal cell connections is thus much higher in the slice. The analysis of the divergence of CA3 cells on themselves illustrates the connectivity rule in the whole structure (Fig. 11c). Proximal cells give rise to few connections (500) whereas mid and distal cells provide the majority of synapses (2,100–2,600).

Finally, we investigated the number of shared associational inputs in the whole structure and in the slice for three CA3 neurons (y = 200) located in the proximal, mid, and distal parts along the transverse axis. In the whole structure, the proximal cell (x = 3) receives 2,430 associational inputs and shares them preferentially with proximal cells (55, 2.2%). The number of shared inputs slowly decreases toward the distal end (38, 1.5%) as can be seen on Figure 12a. For the mid (x = 60, 2,336 inputs, Fig. 12b) and distal (x = 119, 2,111 inputs, Fig. 12c) puts the number of shared inputs seems to be identical [50 (2.2%) and 45 (2.1%), respectively]. The same trend is found in the slice where the proximal cell (Fig. 12d) receives 262 inputs with an average sharing of 8 (3%), the mid cell (Fig. 12e) receives 267 inputs with an average sharing of 8 (3%), and the distal cell (Fig. 12f) receives 215 inputs with an average sharing of 7 (3.3%).

From these results it appears that 1) the architecture creates local circuits which are different according to their transverse location; 2) a given cell informs its close neighbours about its activity, i.e., the activity is constrained locally but 3) the associational pathway is very diffuse in terms of local activity since the number of shared inputs is very low (around 3%). This is to be compared with the values obtained for the Schaffer collateral pathway where the activity is more structurated locally. Finally, whereas distal cells receive fewer associational inputs than proximal cells, the low number of shared inputs ensures a global balance of the transmission of associational activity.

We then performed a parametric study to test the robustness of the model. To characterize any change in the connectivity pattern we plotted the number of connections made by the whole CA3 pyramidal cell population on a string of CA3 pyramidal cells along the transverse direction (y = 200 for all these cells). The results are summarized on Figure 13. Variations of G33_1 and G33_2, which control the dispersion of the Gaussian distributions toward the septal and temporal ends, respectively, change the number of inputs without greatly affecting the spatial distribution of the synapses (Fig. 13a–h). The number of inputs increases to reach a maximum for cells located in the first quarter along the string and then decreases. Variations of G33_31 causes only very slight changes in the number of synapses (Fig. 13m–p) since it controls the dispersion along the transverse axis for the most proximal cells which are very few. Outside the most proximal area CA1 pyramidal cells have a much larger connectivity field along the transverse axis. For this reason variations of G33_32

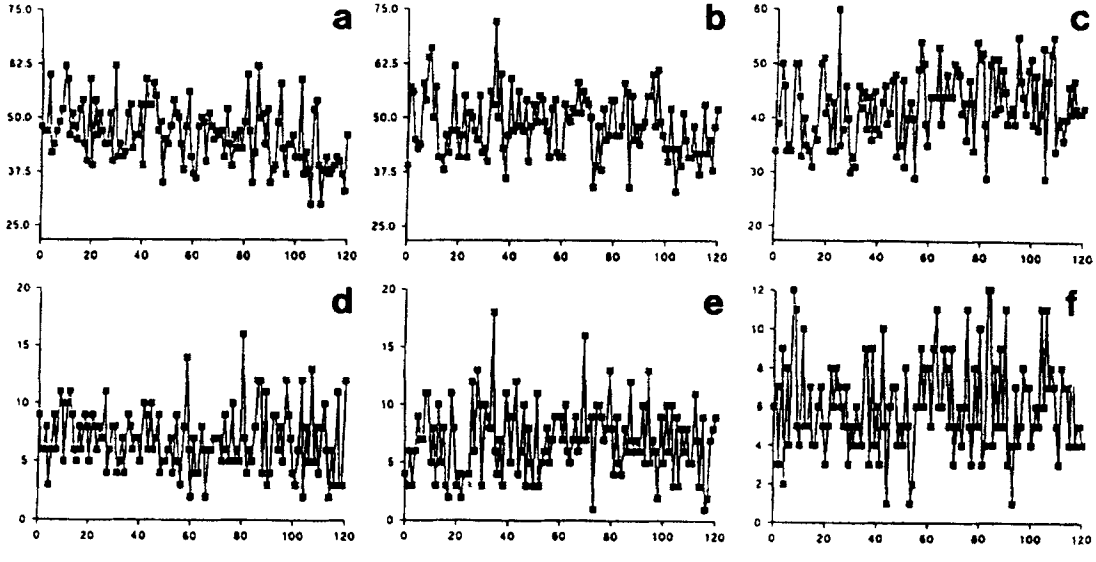

Fig. 12. Number of shared inputs along the transverse axis for a proximal **(a)**, a mid **(b)**, and a distal CA3 cell **(c)** in the whole hippocampus. In **a**, x = 3. The cell is sharing more inputs with its nearest neighbors. In **b** x = 60. This cell shares equally its inputs with all its neighbors. In **c**, x = 119. The shape is a mirror image of that in a, i.e. the cell shares more inputs with its nearest neighbors in the distal part **d–f** as a–c for a slice. Note the similarity of patterns. The set of parameters was G33_1 = 90, G33_2 = 40, G33_31 = 10, G33_32 = 200, and p33 = .03.

drastically affect the number of connections since with a wide dispersion more neurons can be contacted. The shape of the curve is not changed, but the discrepancy between proximal and distal ends is more apparent for certain values (Fig. 13n,o). As could be expected, changes in p33, which directly controls the probability of finding a connection, affect the number of synapses without changing the general characteristics of the connectivity pattern (Fig. 13q–t).

As previously stated, the CA3 pyramidal cell/CA3 interneuron pathway is equivalent, from a modeling point of view, to the CA3 pyramidal cell/CA3 pyramidal cell pathway.

CA1 associational pathway

The probability of finding functional CA1 pyramidal associational connections is very low (Thomson and Radpour,

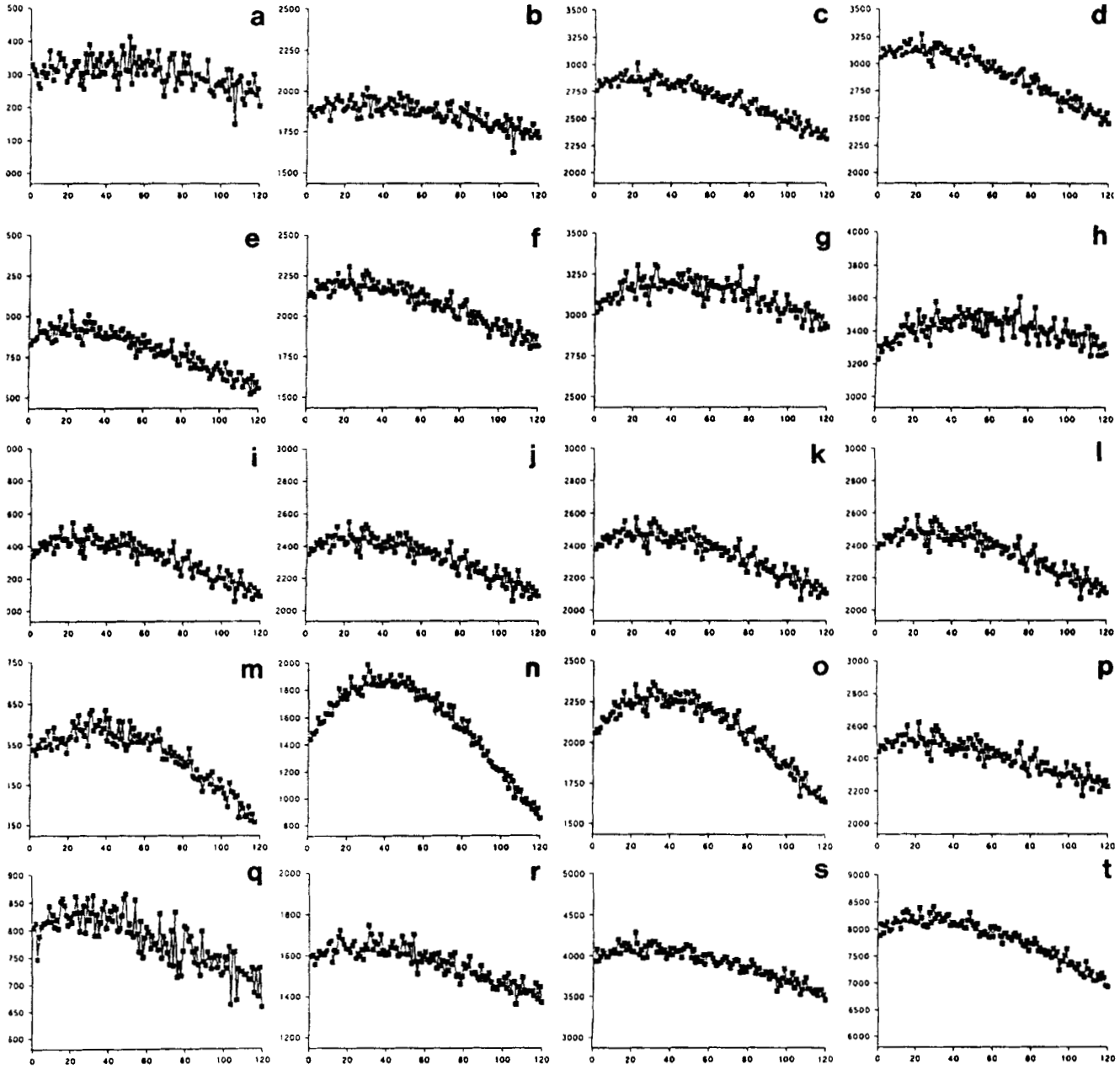

Fig. 13. Variation in the number of CA3 to CA3 connections (as in Fig. 11a) as a function of the different parameters. The basic set of parameters was G33_1 = 90, G33_2 = 40, G33_31 = 10, G33_32 = 200, and p33 = .03 and we varied one parameter at a time. **a:** G33_1 = 30. **b:** G33_1 = 60. **c:** G33_1 = 120. **d:** G33_1 = 150. **e:** G33_2 = 10. **f:** G33_2 = 25. **g:** G33_2 = 90. **h:** G33_2 = 120. **i:** G33_31 = 3. **j:** G33_31 = 5. **k:** G33_31 = 20. **l:** G33_31 = 40. **m:** G33_32 = 50. **n:** G33_32 = 100. **o:** G33_32 = 300. **p:** G33_32 = 400. **q:** p33 = .01. **r:** p33 = .02. **s:** p33 = .05. **t:** p33 = .1. The general spatial distribution of synapses is not changed since the shape of the curve is unchanged apart from a more well-marked peak for certain values. As could be expected the only modified variable is the number of synapses.

1991). Moreover, unlike those found in CA3 area (Ishizuka et al., 1990), *P. vulgaris* leucoagglutin injections in CA1 do not show clear patterns of connectivity (Amaral et al., 1991).

As a first approximation we consider three classes of CA1 pyramidal cells according to their pattern of connectivity. The most proximal ones (class 0) project with a dispersion angle of 90° toward the distal end. The probability of finding a connection is p11_0. CA1 pyramidal cells located in the mid part along the transverse axis (class 1) project locally in a circular area (200 μm radius) and then with a dispersion angle of 90° toward the distal end. For the two patterns the respective probabilities are p11_11 and p11_12. Finally, the most distal cells (class 2) project backwards with a dispersion angle of 90° toward the proximal end. The point from which the dispersion occurs is located in the subiculum and its location depends upon the transverse location of the emitting CA1 pyramidal cell. CA1 cells located at the border of the subiculum project just across into it whilst cells located far away project deeply into it. The corresponding probability is p11_2. The partition of the three classes depends upon G11 which controls the dispersion of a Gaussian distribution.

The results presented hereafter were obtained with the following set of parameters: G11 = 4, p11_0 = .01, p11_10 = .02, p11_11 = .01 and p11_2 = .01.

The results of the simulation of a *P. vulgaris* leucoagglutin injection experiment are shown on Figure 14. Three areas were labeled respectively in the proximal, mid and distal part along the transverse axis in the middle part of the CA1 area along the longitudinal axis. The figure indicates clearly that the distribution of synapses is even in the projecting area. This could be expected as the connections are chosen randomly in a uniform manner. On Figure 15a we plotted the number of CA1 associational connections received by CA1 pyramidal cells located on a string parallel to the transverse axis (Y = 270 for all these cell) from the whole CA1 pyramidal cell population. The number of connections rises slowly from 0 to a maximum of 3,200 (which corresponds to a probability of 3,200/318,600 = 1%). From this graph it is clear that proximal cells receive very few associational fibres whereas the highest probability of connections is found near the subiculum. Figure 15b is the corresponding figure for a slice. There is a similar pattern of connectivity and the maximum number of connections for the most distal cells is 180, which corresponds to a probability of 1.12%. The CA1 associational pathway seems to spread out information the same way as that in CA3. In Figure 15c we plotted the divergence of a string of CA1 pyramidal cells in the whole structure. Proximal cells provide the majority of synapses whereas distal ones provide a minimum number because their pattern of backward projection is very limited. The jumps in the curve indicate that at some distance class 1 cells which project toward the distal end and thus have a restricted connectivity field coexist with class 2 cells which project toward far subiculum and thus project further backward in CA1 with a large connectivity field. Finally, we investigated the number of shared inputs for a proximal (X = 5, Fig. 15d), mid (X = 59, Fig. 15e), and a distal CA1 cell (X = 110, Fig. 15f) located in the mid part of the longitudinal axis (Y = 270). The proximal cell shares very few inputs (1.8%) with the

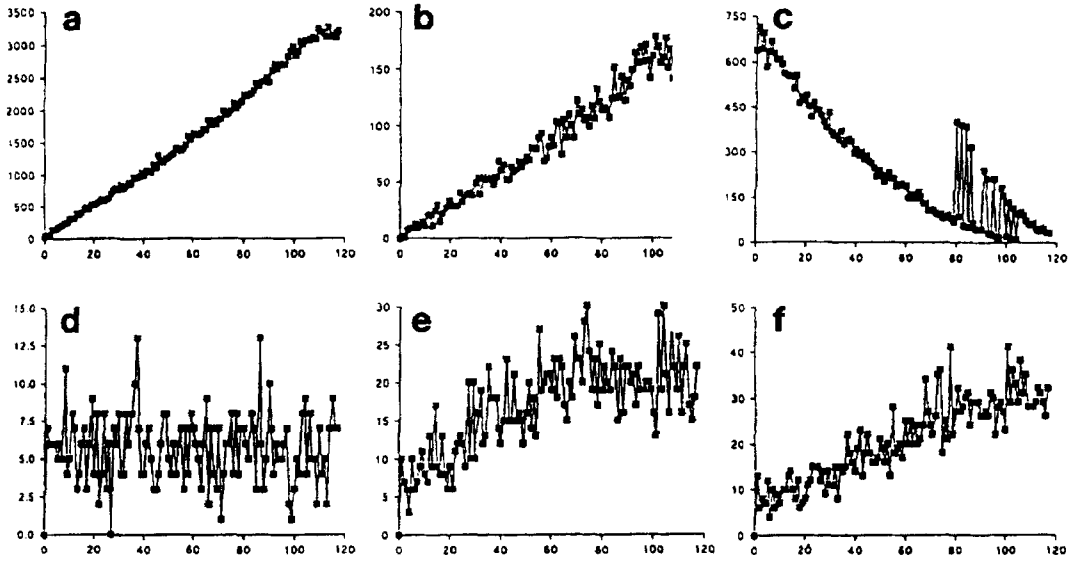

Fig. 15. **a:** Convergence from CA1 to CA1. This graph shows the evolution of the number of pyramidal cells in the whole CA1 area contacting a given CA1 pyramidal cell in the mid septotemporal part of the hippocampus as a function of the transverse location of the receiving CA1 pyramidal cell (Y = 270 for all these cells). The convergence increases linearly toward the distal end of the CA1 area. **b:** Same as a but for a slice. Note that the connectivity pattern is unchanged. **c:** Divergence from CA1 to CA1. This graph shows the evolution of the number of CA1 pyramidal cells a given CA1 pyramidal cell is contacting as a function of the transverse location of the emitting CA1 pyramidal cell. The number of synapses decreases toward the subiculum. The jumps correspond to different rules of connectivity. Number of shared inputs along the transverse axis for a proximal **(d),** a mid **(e),** and a distal cell **(f).** In d, X = 5. The cell is sharing very few inputs with its nearest neighbours. In e X = 59. This cell shares more of its inputs with its close neighbours as in f where X = 110. The set of parameters was G11 = 4, p11_0 = .01, p11_10 = .02, p11_11 = .01 and p11_2 = .01.

CA1 pyramidal cells located on a transverse string. For the mid and distal cells the sharing decreases toward the proximal end to reach 1.4% and 1.1%, respectively.

These results show that the CA1 associational pathway is even more diffuse than the CA3 associational pathway and that the highest density of associational connections is located near the subiculum. With the rule and parameters used in this simulation it is clear that 1) the area of highest probability of finding CA1 pyramidal cells–CA1 pyramidal cells connections is near the subiculum and 2) CA1 pyramidal cell collaterals have a global structurating effect rather than a local one on the incoming activity.

The CA1 pyramidal cell/interneuron pathway issue can be seen as a part of the CA1 pyramidal cell/CA1 pyramidal cell one, with a lower density of neurons. The same general conclusions can be drawn.

Finally, the parametric study (data not shown) is straightforward since it will only affect the number of synapses without changing the general conclusions concerning the different septotemporal and transverse gradients of connectivity.

Interneuron/pyramidal cell connections

Since very few data are available about the connectivity field of the axonal arborization of CA3 and CA1 interneurons we adopted the following general model for all classes of interneurons: The connectivity field is represented by an ellipsoidal field the centre of which is occupied by the interneuron. Inside this ellipsoidal field we defined a matrix of connectivity which elements represented the probability of finding an axonal branch at a given longitudinal/transverse direction. This matrix was built similarly to that for the CA3–CA1 projection (see Fig. 3). In this situation, I is the longitudinal axis and J is the transverse axis. The dispersion of the two Gaussian distributions (one for each axis) is given by GIE_1 and GIE_2, respectively. If one wants a uniform distribution in the ellipsoidal field it is sufficient to give these two parameters high values (>500). For intermediate ones (50–200) the probability of finding an axonal collateral decreases with the distance from the interneuron in all directions. The other parameters are A and B, the lengths of the two axes of the ellipse along the transverse and the longitudinal axes, respectively, and pIE is the probability of establishing a connection between a pyramidal cell and an interneuron. The same procedure is applied for all classes of interneurons in both CA1 and CA3 areas. To illustrate this we present the connectivity pattern found between one class of CA1 interneurons and CA1 pyramidal cells. We consider 4,060 interneurons in the whole structure (29 along the transverse axis and 140 along the longitudinal axis) evenly scattered among the whole population of CA1 pyramidal cells (318,600 neurons) and the following set of parameters: GIE_1 = 100, GIE_2 = 100, A = 500 μm, B = 750 μm, and pIE = .5.

An interneuron located in the middle part of CA1 area (with respect to both longitudinal and transverse axes) has an elliptic axonal field containing 27,565 CA1 pyramidal cells, and the number of contacted cells is 12,989 in the whole structure. An interneuron thus affects the dynamics of a considerable number of pyramidal cells. Their dendritic arborization is much less extensive than their axonal field. As a consequence, inputs from external afferents (Schaffer collaterals, for example) which will activate a subset of interneurons and pyramidal cells will also contribute to the inhibition of pyramidal cells far outside their activated field. As a consequence the stimulation of a bundle of afferent fibres will create an area of mixed excitation and inhibition. Excitation will be constrained inside the field defined by the activated fibres, which, in turn, will be surrounded by a wide area of inhibition. We now consider a string of CA1 pyramidal cells along the transverse axis (Y = 270). Each neuron receives 170 terminals from different interneurons in the whole structure and 25 in the slice. The activity of a pyramidal cell is thus highly controlled by interneurons in the slice (12% of the interneuron population). The number of inhibitory inputs shared in the slice is also very important as each cell shares 25% of its inhibitory inputs with its neighbours along a string parallel to the transverse axis. As a consequence interneurons may act as a global filter transforming the incoming activity and distributing it to a large population of CA1 pyramidal cells thus ensuring a certain amount of coherence (see Discussion). The parametric study is straightforward as the different parameters directly affect the number of connections and their spatial dispersion. The case for interneuron–interneuron connections is again equivalent.

DISCUSSION

This study is an attempt to construct realistic connectivity matrices between the different neuronal populations in CA3 and CA1 areas of the hippocampus of young male Wistar rats. Most single neuron models try to include numerous neurobiological parameters (Segev et al., 1989; Traub et al., 1991b). However, it has been emphasized recently that, apart from the synaptic weights, the most important parameter for the dynamics of a given neuronal network is the mean firing rate of neurons and that neural network behaviours are independent from the way individual neurons are modeled (Gerstner and Van Hemmen, 1992). It must be stressed that this result is valid for a single class of neuronal networks, i.e., the fully connected recurrent networks of the Hopfield type (Hopfield, 1982, 1984). However, Hopfield type networks do not seem to exist in vivo.

It is obvious that the space of states of a system is considerably reduced if strong constraints are imposed on its parameters. Such is the case with connectivity. It has been shown recently how the interpretation of some experiments becomes very difficult if one does not take into consideration the circuitry and how it can lead to opposite conclusions (Claiborne et al., 1993). This problem is even more acute when one analyses information processing and the dynamics in a neuronal network. It has been shown in the cerebellar cortex how strict connectivity rules impose very strong constraints on the dynamics of a network and how this, in turn, can lead to complex behaviours which could not be determined intuitively (Bernard and Axelrad, 1991; Bernard et al., 1993). Some of these theoretical results were verified experimentally (Bernard and Axelrad, 1993).

Our own approach is based on interaction between experimental and theoretical data. For this reason we felt that it was necessary to build a realistic model of hippocampal circuitry which may be used to simulate either the hippocampal slice or

as a reasonable approximation of the whole hippocampal structure. The predictive values which might be obtained subsequently are highly dependent upon the set of parameters used to build the different connectivity matrices. It is the choice of these parameters that we will now discuss.

Synaptic model

It is not the purpose of this study to discuss a model of a single neuron. However, in our simulations we apply for each connection a certain set of values which play a fundamental role in the dynamics of individual neurons at each synaptic site. There are the synaptic weight, the probability of activation of the synapse, the spatial location of the synapse in the dendritic tree, as well as the different ionotropic receptors involved. The location of the different synapses in the dendritic tree is a fundamental issue since distal and proximal inputs are known to have different kinetics (Williams and Johnston, 1991). The values produced by the model approximate the locus of projection. They are derived from anatomical data which presently can only provide gross general rules. The exact pattern of connectivity for the majority of efferent neurons still needs to be investigated in detail. Moreover, the values we provide must be adapted to the single neuron model used. Multicompartmental models with active channels are now commonly used (Lytton and Sejnowski, 1991; Traub et al., 1991b; Traub and Miles, 1991) and the transformation is thus more straightforward since each compartment represents a specific location in the dendritic tree. More compartmental models are taking into account the complex branching patterns of the dendrites (Major et al., 1993; Spruston et al., 1993; Stockley et al., 1993). This is important since spiking and bursting events are known to occur in apical dendrites (Wong et al., 1979; Bernardo et al., 1982; Turner et al., 1991, 1993, Wong and Stewart, 1992; Jaffe et al., 1992; Colling and Wheal, 1993).

One present limitation of our model is that it does not yet provide a real 3D projecting pattern onto the dendritic tree. The only dimension we consider is the axis perpendicular to both transverse and longitudinal axes. In order to obtain a more realistic 3D location of the synapses, along both transverse and longitudinal directions, more anatomical data are needed. In particular, it would be necessary to build generic models of dendritic and axonal fields from 3D reconstructions of labeled neurons. This has recently been done in the dentate gyrus (Halasy and Somogyi, 1993; Han et al., 1993) and hopefully should soon be extended to CA3 and CA1 regions. Likewise, it would be helpful to have more data from labeled CA3 pyramidal cells in vivo in order to determine the general rules of branching of Schaffer collaterals that take into account the connectivity gradients (Koch and Zador, 1993; Li et al., 1993). With access to such data it would be possible to construct a more realistic 3D connectivity pattern. The same proposal applies for the axonal fields of all types of neurons.

There are also numerous unresolved issues about the activation of different types of receptors (NMDA and AMPA or $GABA_A$ and $GABA_B$). In particular, we do not know if they are colocalized and/or if they are activated by different sets of synapses etc. As a first approximation, we colocalized them when two sets of receptors were activated experimentally. More refined electrophysiological data should clarify this point. Another problem stems from the range and complexity of the different phenomenon that might occur at or near the synaptic site. For example, zinc or neurotransmitters such as norepinephrine and serotonin are involved in the control of GABA receptors (Oleskevich and Lacaille, 1992; Ropert and Guy, 1991; Cohen et al., 1992; Segal, 1990b; Doze et al., 1991; Xie and Smart, 1993), not to mention the presynaptic modulation by many neurotransmitters including GABA (Thompson et al., 1993). Likewise, we have not included the different metabotropic receptors in our model since, although they may be involved in the induction of long-term potentiation and depression (Bashir et al., 1993a, b; Liu et al., 1993; Miles and Poncer, 1993), their functional role is yet to be determined. Hopefully, a more detailed model of single neurons taking into consideration their functional characteristics (Schoepp et al., 1990; Tanabe et al., 1992, 1993) and spatial distribution will emerge.

Finally, each synapse is characterised by its probability of activation. This value is derived from paired electrophysiological recordings and represent in our model not only the failure of synaptic transmission but also the failure of spike transmission at branching points along the axon.

Schaffer/commissural pathway

Since ideal data about the exact 3D pattern of projection of Schaffer collaterals are not available (Tamamaki and Nojyo, 1991; Li et al., 1993), we have used the results of *P. vulgaris* leucoagglutin injection experiments (Ishizuka et al., 1990) to generate gross anatomical rules for these projections. Our own simulations of these experiments give similar patterns of projections. We used the connectivity matrix thus created to perform some statistical analysis on synaptic divergence, convergence, and connectivity. In the model of a 400 μm thick slice the number of direct connections from CA3 to mid-CA1 pyramidal cells is 580. This data raises two issues. The estimated number of 100–300 simultaneously activated synapses required to make a CA1 pyramidal cell discharge (Sayer et al., 1989; Andersen, 1990) corresponds in a slice to the activation of 1/6 to 1/2 of the population of CA3 pyramidal cells which synapses with an individual CA1 pyramidal cell. If we assume that 100 synapses are sufficient to activate a cell, there are ${}_{580}C_{100} = 580!/100!\times480! \approx 2.7 \times 10^{114}$ possible combinations. In the whole structure we obtain a value of ${}_{8,000}C_{100}$ which is considerably higher than in the slice. To put these large numbers into perspective, the estimated number of particles in the universe is 10^{75}. We have shown that the degree of convergence is dependent upon the longitudinal thickness of CA3/CA1 areas. Proportionately more inputs are involved when studying the behaviour of reduced volumes of tissue along the longitudinal axis. This result supports the lamellar hypothesis, even if the pathway is less parallel than previously thought (Andersen et al., 1971). Despite the septotemporal divergence of this pathway (Ishizuka et al., 1990), which was used as an argument against the lamellar hypothesis (Finch et al., 1983; Amaral and Witter, 1989), there is still some parallelism as confirmed by recent HRP studies (Tamamaki and Nojyo, 1991; Li et al., 1993). The study of the number of shared inputs confirmed the latter statement. In the slice a given CA1 pyramidal cell shares an average of 10% of its inputs with its neighbours. However, we must stress that the set of common inputs is different from one

neighbour to the other. If we assume that there is a sufficient amount of excitation from the ipsilateral CA3 pyramidal cells to make a given CA1 pyramidal cell discharge, this same activity will be sufficient to make several neighbouring CA1 pyramidal cells discharge within the slice. If we look at the whole structure the activity will be shared more diffusely as the proportion of shared afferents drops to 7%.

The model also clearly identified gradients of connectivity in the transverse directions. The area which receives the larger amount of activity and which shares it with the rest of the CA1 pyramidal cell population corresponds to the mid part of the transverse axis. However, the number of shared inputs is greater with proximal and mid cells wherever the CA1 pyramidal cell is located. Thus, despite the divergence brought about by septotemporal and transverse gradients, the Schaffer collateral pathway is partly organised in a lamellar-like way. This means that a narrow band (with respect to the longitudinal direction) of CA1 pyramidal cells will receive many correlated signals and thus produce a high degree of cooperativity. We also found a transverse gradient since activity is preferentially shared in the proximal and distal parts of CA1 area. Likewise, CA1 pyramidal cells along the transverse axis do not seem to play the same functional role since mid cells receive more activity than the others. These predictions could be verified with an entropy analysis (Bernard et al., 1993) in a dynamic model of a slice.

At the present we do not know if the number of spines on the dendritic tree of CA1 pyramidal cells vary according to their transverse location. The model shows such a gradient since mid CA1 pyramidal cells receive more Schaffer collateral inputs than cells located at the edges of the CA1 area. Moreover, the locus of projection varies greatly (from lower oriens to upper radiatum) according to the transverse location of the emitting CA3 pyramidal cell. Thus, we also expect gradients in the number of synapses in the different parts of the dendritic tree according to the transverse location of the CA1 pyramidal cells. However, fewer Schaffer collateral inputs could also be balanced by a greater number of commissural connections (which is not the case in our model), more dense CA1 associational connections, which seems to be the case in distal CA1 (Amaral et al., 1991), and/or a greater number of extrahippocampal inputs. In our model we have considered that all CA3 Schaffer collaterals follow the same connectivity rule. However, it is known that at least half of the CA3 pyramidal cell population lack Schaffer collateral proper (Lorente de Nó, 1934; Blackstad, 1985; Ishizuka et al., 1990). These cells might follow a different connectivity rule and balance out the different transverse gradients observed in the number of synapses and information processing. A more detailed HRP study might address this issue. Likewise, we have considered that commissural fibres have the same connectivity pattern as the Schaffer one on the basis of gross anatomical considerations (Gottlieb and Cowan, 1973; Laurberg, 1979; Chan, 1992). Again differences might balance out the gradients.

We also have taken into account the patterns of projection in both stratum oriens and radiatum. This is an important parameter since it has been reported recently that basal and apical dendrites of CA1 pyramidal cells do not have the same properties following tetanic stimulation (Kaibara and Leung, 1993).

Finally, all these results are fairly robust as demonstrated by the parametric study and thus do not seem to be the product of a specific set of parameters.

CA3 associational pathway

Again we used data from *P. vulgaris* leucoagglutin injection experiments (Ishizuka et al., 1990) to model CA3 associational pathway. Modeling these experiments gives similar results. The connectivity matrix we built is thus not based on detailed 3D reconstructions of CA3 pyramidal cell axonal collaterals because such data are not available. However, this simplified model already gives interesting predictive values in terms of distribution of synapses and local divergence and convergence of activity.

The lamellar organisation is even more important than the one found for the Schaffer collateral pathway. Even if the collaterals project quite far in the longitudinal directions a great number of connections are found within the thickness of a slice. Proximal cells which provide the minimum number of associational connections receive the maximum number of such connections. These important transverse gradients suggest that associational activity will not be distributed in a uniform fashion. The sharing of inputs is very diffuse even in a lamella (3%) and is generally constrained locally following a vicinity relationship. As a consequence, information is distributed in a diffuse way despite the impressive connectivity pattern of the CA3 associational pathway. This may not be so surprising since it has been shown that a comparable pathway in the cerebellar cortex, the Purkinje cell axonal collaterals, which is even more diffuse, imposes very strict constraints on the space of states of the system and greatly enhances its informational content (Bernard et al., 1993). A densely distributed system is thus not absolutely necessary for the transmission of information even over long distances (Bernard et al., 1993). We expect that this will also be the case for the CA3 associational pathway. Again an entropy analysis in a dynamic model is in order. If the analogy with the Purkinje cell axonal collateral system holds, the role of the CA3 associational pathway would be to ensure local coherence of information before relaying it to CA1 pyramidal cells. Moreover, the diffuse aspect of the excitatory CA3 associational pathway is not surprising since too much mutual excitation might saturate the system.

Associational synapses are distributed from lower oriens to upper radiatum. At the present it is not known if these different parts of the dendritic tree are functionally very different.

Finally, the parametric study confirmed the robustness of the results.

CA1 associational pathway

Phaseolus vulgaris leucoagglutin injection experiments were more difficult to analyze in terms of projection patterns (Amaral et al., 1991) and therefore we had to make more assumptions. Even if electrophysiological data show very few CA1 associational connections (Thomson and Radpour, 1991), it is possible that more associational synapses exist and that they exert subtle control without giving rise to measurable postsynaptic potentials. More precise 3D reconstructions of CA1 pyramidal cell axonal collaterals at various locations along the transverse axis are necessary to build realistic connectivity matrices. Nevertheless, our modeling of *P. vulgaris*

leucoagglutin injection experiments show very similar results to those obtained experimentally.

We have found an important gradient of connectivity since distal CA1 pyramidal cells receive a maximum number of associational connections and proximal cells receive a minimum. This can be compared with the observation that proximal CA1 cells in a lamella receive more inputs from CA3 pyramidal cells than distal ones. There thus seems to be a natural balancing in the connectivity gradients.

As for the two preceding pathways the longitudinal and transverse gradients are coupled to gradients in the projection area (from oriens to radiatum). Their relevance to information processing at the cell levels remains to be determined.

In this case the parametric study also showed the robustness of the results.

Interneuron/pyramidal cell pathway

More refined experimental techniques are now currently used to provide better insights on the anatomical and electrophysiological characteristics of interneurons in the hippocampus (Han et al., 1993; Gulyás et al., 1993a,b). However, owing to the lack of precise 3D reconstructions of the dendritic and axonic fields of the different classes of interneurons we again have had to make more assumptions. The general pattern of the axonal field was represented by an ellipse inside which the probability of a connection with any neuron decreases with the distance from the interneuron. We based this model on the available anatomical data (Lacaille et al., 1987; Lacaille and Williams, 1990; Lacaille and Schwartzkroin, 1988a; Kawaguchi and Hama, 1987, 1988, Schwartzkroin and Kunkel, 1985; Kawaguchi et al., 1987; Li et al., 1992). The two parameters controlling the extension of the axonal field are the long and short axis of the ellipse. We have assumed as a first approximation that they are parallel to the longitudinal and transverse axes. However, we have seen that both Schaffer/commissural and CA3 associational pathways are organised along axes which are not parallel to these axes. Intuitively, we would expect the axes of the ellipse to be aligned along I and J axes. If 3D reconstructions confirm this point the change in the software will be straightforward since it will be sufficient to rotate the connectivity matrix by the appropriate angle. Obviously, each class of interneurons has its own set of parameters. But the problem is becoming even more complex as more classes of interneurons are characterized (Soriano and Frotscher, 1993; Gulyás et al., 1993a). A fortiori it is not known if these different classes of interneurons have unique connectivity fields. However, we took into account the locus of projection in the dendritic trees of the cells they contact. A dynamic model should demonstrate possible functional differences according to the locus of projection of each class of interneuron as it is expected that each class participates differently in the balance of excitation and inhibition and thus to the tuning of the behaviour of the neurons they contact.

A general connectivity feature is the large extension of the axonic field, more particularly, in the longitudinal direction. This may have very important functional properties. Let us consider an afferent volley arriving through a subset of mossy fibres. This volley would be spatially constrained since the mossy fibre pathway is characterized by a lamellar organization (Blackstad et al., 1970; Swanson et al., 1978) and it would activate a lamella of CA3 pyramidal cells. The activated neurons will in turn inform their neighbours about their activity through the CA3 associational pathway. Simultaneously, interneurons will be activated and will create a halo of inhibition which will extend deep in the longitudinal direction. In CA3 we will thus have a lamella in which strong excitation of pyramidal cells and interneurons can occur surrounded by an area where subtle processes of inhibition/excitation/disinhibition will occur. This area will be in turn surrounded by a pure inhibitory halo.

This architecture ensures that pyramidal cells in a lamella will receive multiple contacts from the different interneurons (12% of the whole population). Together with convergent inhibitory pathways the sharing of inputs is very important (25%). The interneuron network thus seems to establish a higher degree of coherence through inhibitory signals than that brought about by the more diffuse excitatory associational pathway. However, the significance of this architectural organization is yet to be investigated in a model in which "relevant" afferent signals will be introduced.

CONCLUSIONS

To our knowledge, this is the first connectivity model of CA3 and CA1 areas of the hippocampus incorporating the maximum amount of known electrophysiological and anatomical data. We hope that it will be helpful to both modelers and experimentalists. We have been particularly keen to show the different gradients of connectivity and their effects on the convergence, divergence, and distribution of activity. In particular, these gradients show that the sets and number of synapses activated by afferent signals will be totally different depending upon the locus of activation and according to the experimental conditions used (in vivo or in vitro recordings).

We suggest that despite a high degree of divergence the Schaffer/commissural pathway is still organized in a lamellar fashion from an information processing point of view. Both CA3 and CA1 associational pathway are more diffuse and might produce local coherence of the incoming activity. Finally, interneurons with the large inhibitory halo they generate might impose even stronger spatial constraints on information by preventing its diffusion in the network.

The differences found in the distribution of inputs between the slice and the whole structure indicate that one has to be very careful when generalising functional properties from one structure to the other.

These connectivity matrices will now be incorporated into a network model of the slice or indeed of the whole hippocampus (Ge et al., 1992, 1993; Willis et al., 1993). This model will be used to simulate the role of connectivity in the generation of epileptiform activity. It will also be possible to simulate and analyse how signals are distributed and processed in the different neuronal elements of CA3 and CA1 as well as other models of synaptic plasticity.

ACKNOWLEDGMENTS

The authors wish to express their sincere thanks to P. Andersen, N. Best, J. Jefferys, J.-C. Lacaille, R. Miles, J. O'Keefe, and M. Witter for the help and suggestions they provided. This study was supported by the Wellcome Trust, SERC, and OTAN.

REFERENCES

Alger B (1984) Characteristics of a slow hyperpolarizing synaptic potential in rat hippocampal cells in vitro. J Neurophysiol *52*:892–910.

Alger B, Nicoll R (1980) Spontaneous inhibitory postsynaptic potentials in hippocampus: mechanism for tonic inhibition. Brain Res *200*:195–200.

Alger B, Nicoll R (1982a) Feed-forward dendritic inhibition in rat hippocampal cells studied in vitro. J Physiol (Lond) *328*:105–123.

Alger B, Nicoll R (1982b) Pharmacological evidence for two kinds of GABA receptors on rat hippocampal pyramidal cells studied in vitro. J Physiol (Lond) *328*:125–141.

Amaral D (1978) A Golgi study of cell types in the hilar region of the hippocampus in the rat. J Comp Neurol *182*:851–914.

Amaral D, Witter M (1989) The three-dimensional organization of the hippocampal formation: a review of anatomical data. Neuroscience *31*:571–591.

Amaral D, Ishizuka N, Claiborne B (1990) Neurons, numbers and the hippocampal network. Prog Brain Res *83*:1–11.

Amaral D, Dolorfo C, Alvarez-Royo P (1991) Organization of CA1 projections to the subiculum: a PHA-L analysis in the rat. Hippocampus *1*:415–436.

Andersen P (1990) Synaptic integration in hippocampal CA1 pyramids. In: *Progress in brain research*, Vol. 83 (Zimmer J, Ottersen O, eds.), pp 215–222. New York: Elsevier.

Andersen P, Blackstad T, Lomo T (1966) Location and identification of excitatory synapses on hippocampal pyramidal cells. Exp Brain Res *1*:236–248.

Andersen P, Bliss T, Skrede K (1971) Lamellar organization of hippocampal excitatory pathways. Exp Brain Res *13*:222–238.

Andersen P, Silfvenius H, Sundberg S, Sveen O, Wigstrom H (1978) Functional characteristics of unmyelinated fibres in the hippocampal cortex. Brain Res *144*:11–28.

Andersen P, Blackstad T, Hulleberg G, Vaaland J, Trommald M (1987) Dimensions of dendritic spines of rat dendate granule cells during long-term potentiation (LTP). J Physiol (Lond) *390*:264p.

Andreasen M, Lambert J, Jensen M (1989) Effects of the new non-N-methyl-D-aspartate antagonists on synaptic transmission in the in vitro rat hippocampus. J Physiol (Lond) (Abstr) *414*:317–336.

Ashwood TJ, Lancaster B, Wheal HV (1984) In vivo and in vitro studies on putative interneurones in the rat hippocampus: possible mediators of feed-forward inhibition. Brain Res *293*:279–291.

Babb T, Pretorius J, Kupfer W, Brown W (1988) Distribution of glutamate-decarboxylase-immunoreactive neurons and synapses in the rat and monkey hippocampus: light and electron microscopy. J Comp Neurol *278*: 121–138.

Baimbridge K, Miller J, Parkes C (1982) Calcium-binding protein distribution in the rat brain. Brain Res *239*:519–525.

Bashir ZI, Bortolotto ZA, Davies CH, Berretta N, Irving AJ, Seal AJ, Henley JM, Jane DE, Watkins JC, Collingridge GL (1993a) Induction of LTP in the hippocampus needs synaptic activation of glutamate metabotropic receptors. Nature *363*:347–350.

Bashir ZI, Jane DE, Sunter DC, Watkins JC, Collingridge GL (1993b) Metabotropic glutamate receptors contribute to the induction of long-term depression in the CA1 region of the hippocampus. Eur J Pharmacol *239*:265–266.

Bekkers J, Stevens C (1989) NMDA and non-NMDA receptors are co-localized at individual excitatory synapses in cultured rat hippocampus. Nature *341*:230–233.

Bernard C, Axelrad H (1991) Propagation of parallel fiber volleys in the cerebellar cortex: a computer simulation. Brain Res *565*:195–208.

Bernard C, Axelrad H (1993) Effects of recurrent collateral inhibition on Purkinje cell activity in the immature rat cerebellar cortex. An in vivo electrophysiological study. Brain Res *626*:234–257.

Bernard C, Axelrad H, Giraud B (1993) Effects of collateral inhibition in a model of the immature rat cerebellar cortex: multineuron correlations. Cog Brain Res *1*:100–122.

Bernardo L, Masukawa L, Prince D (1982) Electrophysiology of isolated hippocampal dendrites. J Neurosci *2*:1614–1622.

Best N, Mitchell J, Wheal H (1993a) Ultrastructure of parvalbumin-immunoreactive neurons in the CA1 area of the rat hippocampus following a kainic acid lesion. Acta Neuropathol (Berl) *87*:187–195.

Best N, Mitchell J, Wheal H (1993b) Ultrastructure of parvalbumin-immunoreactive neurons in the CA1 area of the rat hippocampus following a kainic acid lesion. Brain Res Assoc Abstr *10*:9.

Blackstad T (1985) Laminar specificity of dendritic morphology: examples from the guinea pig hippocampal region. In: *Quantitative neuroanatomy in transmitter research* (Agnati L, Fuxe K, eds.), pp 55–69. London: Macmillan.

Blackstad T, Brink K, Hem J, Jeune B (1970) Distribution of hippocampal mossy fibers in the rat. An experimental study with silver impregnation methods. J Comp Neurol *138*:433–450.

Blake J, Brown M, Collingridge G (1988) CNQX blocks acidic amino acid induced depolarizations and synaptic components mediated by non-NMDA receptors in rat hippocampal slices. Neurosci Lett (Abstr.) *89*:182–186.

Bleakman D, Harrison NL, Colmers WF, Miller RJ (1992) Investigations into neuropeptide Y-mediated presynaptic inhibition in cultured hippocampal neurones of the rat. Br J Pharmacol *107*:334–340.

Boss B, Turlejski K, Stanfield B, Cowan W (1987) On the number of neurons in fields CA1 and CA3 of the hippocampus of Sprague-Dawley and Wistar rats. Brain Res *406*:280–287.

Braitenberg V, Schutz A (1990) Some anatomical comments on the hippocampus. In: *Progress in brain research*, Vol. 87 (Storm-Mathisen J, Zimmer J, Ottersen O, eds), pp 21–37. New York: Elsevier.

Braun K, Scheich H, Schachner M, Heizmann C (1985a) Distribution of parvalbumin, cytochrome oxydase activity and 14c-2-deoxyglucose uptake in the brain of the zebra finch. Part 2: visual system. Cell Tissue Res *240*:117–127.

Braun K, Scheich H, Schachner M, Heizmann C (1985b) Distribution of parvalbumin, cytochrome oxydase activity and 14c-2-deoxyglucose uptake in the brain of the zebra finch. Part 1: auditory and vocal motor system. Cell Tissue Res *240*:101–115.

Brown T, Ganong A, Kairiss E, Keenan C, Kelso S (1989) Long-term potentiation in two synaptic subsystems of the hippocampal brain slice. In: *Neural models of plasticity: experimental and theoretical approaches* (Byrne J, Berry W, eds), pp 266–306. San Diego: Academic Press.

Capek R, Esplin B (1991) Attenuation of hippocampal inhibition by a NMDA (N-methyl-D-aspartate) receptor antagonist. Neurosci Lett *129*:145–148.

Chan D (1992) *A topographical analysis of hippocampal field connectivity in the rat. PhD Thesis,* University College London,

Christian E, Dudek F (1988) Electrophysiological evidence from glutamate microapplications for local excitatory circuits in the CA1 area of rat hippocampal slices. J Neurophysiol *59*:110–123.

Claiborne BJ, Xiang Z, Brown TH (1993) Hippocampal circuitry complicates analysis of long-term potentiation in mossy fiber synapses. Hippocampus *3*:115–122.

Cohen GA, Doze VA, Madison DV (1992) Opioid inhibition of GABA release from presynaptic terminals of rat hippocampal interneurons. Neuron 9:325–335.

Colling S, Wheal H (1993) Fast sodium action potentials are generated in the distal apical dendrites of rat hippocampal CA1 pyramidal cells. Neurosci Lett

Collingridge G, Gage P, Robertson B (1984) Inhibitory post-synaptic currents in rat hippocampal CA1 neurons. J Physiol (Lond) *356*:551–564.

Collingridge GL, Herron C, Lester R (1988) Synaptic activation of N-methyl-D-aspartate receptors in the Schaffer collateral-commissural pathway of rat hippocampus. J Physiol (Lond) *399*:283–300.

Danos P, Frotscher M, Freund T (1991) Non-pyramidal cells in the CA3 region of the rat hippocampus: relationships of fine structure, synaptic input and chemical characteristics. Brain Res *546*:195–202.

DeFelipe J, Hendry S, Jones E, Schmechel D (1989) Variability of the terminations of GABAergic chandelier cell axons in the monkey sensory-motor cortex. J Comp Neurol *321*:364–384.

Douglas R, Martin K (1990) Control of neuronal output by inhibition at the axon initial segment. Neural Computation *2*:283–292.

Doze V, Cohen G, Madison D (1991) Synaptic localization of adrenergic disinhibition in the rat hippocampus. Neuron *6*:889–900.

Eichenbaum H, Otto T, Cohen N (1992) The hippocampus what does it do? Behav Neural Biol *57*:2–36.

Finch D, Babb T (1981) Demonstration of caudally directed hippocampal efferents in the rat by intracellular injection of horseradish peroxydase. Brain Res *214*:405–410.

Finch D, Nowlin N, Babb T (1983) Demonstration of axonal projections of neurons in the rat hippocampus and subiculum by intracellular injection of HRP. Brain Res *271*:201–216.

Finnerty GT, Jefferys JGR (1993) Functional connectivity from CA3 to the ipsilateral and contralateral CA1 in the rat dorsal hippocampus. Neuroscience *56*:101–108.

Fraser D, MacVicar B (1991) Low-threshold transient calcium current in rat hippocampal lacunosum-moleculare interneurons: kinetics and modulation by neurotransmitters. J Neurosci *11*:2812–2820.

Freund T, Antal M (1988) GABA-containing neurons in the septum control inhibitory interneurons in the hippocampus. Nature *336*:170–173.

Frotscher M, Zimmer J (1983) Commissural fibers terminate on non-pyramidal neurons in the guinea pig hippocampus—a combined Golgi/EM degeneration study. Brain Res *265*:289–293.

Frotscher M, Leranth C, Lubbers K, Oertel W (1984) Commissural afferents innervate glutamate decarboxylase immunoreactive non-pyramidal neurons in the guinea pig hippocampus. Neurosci Lett *46*:137–143.

Ge Y, Bernard C, Willis J, Wheal H (1992) Transputer modelling of epileptiform activity in the CA1 region of the hippocampus. Am Soc Neurosci *18*:1242.

Ge Y, Willis J, Wheal H (1993) Network bursting synchronized by slow synaptic conductances in rat hippocampus. Brain Res Assoc Abstr *10*:28.

Gerstner W, Van Hemmen JL (1992) Universality in neural networks: the importance of the 'mean firing rate'. Biol Cybern *67*:195–205.

Gottlieb D, Cowan W (1973) Autoradiographic studies of the commissural and ipsilateral association connections of the hippocampus and the dendate gyrus. I. The commissural connections. J Comp Neurol *149*:393–422.

Grinvald A, Manker A, Segal M (1982) Visualisation of the spread of electrical activity in rat hippocampal slices by voltage sensitive optical probes. J Physiol (Lond) *333*:269–291.

Gulyás AI, Miles R, Hájos N, Freund TF (1993a) Precision and variability in postsynaptic target selection of inhibitory cells in the hippocampal CA3 region. Eur J Neurosci *5*:1729–1751.

Gulyás AI, Miles R, Sik A, Tóth K, Tamamaki N, Freund TF (1993b) Hippocampal pyramidal cells excite inhibitory neurons through a single release site. Nature *366*:683–687.

Halasy K, Somogyi P (1993) Subdivisions in the multiple GABAergic innervation of granule cells in the dentate gyrus of the rat hippocampus. Eur J Neurosci *5*:411–429.

Han Z-S, Buhl E, Lorinczi Z, Somogyi P (1993) A high degree of spatial selectivity in the axonal and dendritic domains of physiologically identified local-circuit neurons in the dendate gyrus of the rat hippocampus. Eur J Neurosci *5*:395–410.

Hebb D (1949) *The organization of behavior.* New York: John Wiley.

Heit G, Smith M, Halgren E (1988) Neural encoding of individual words and faces by the human hippocampus and amygdalia. Nature *333*:773–775.

Hestrin S, Nicoll R, Perkel D, Sah P (1990) Analysis of excitatory synaptic action in pyramidal cells using whole-cell recording from rat hippocampal slices. J Physiol (Lond) *422*:203–225.

Hopfield J (1982) Neural networks and physical systems with emergent collective computational properties. Proc Natl Acad Sci USA *79*:2554–2558.

Hopfield J (1984) Neurons with graded response have collective computational properties like those of two states neurons. Proc Natl Acad Sci USA *81*:3088–3092.

Ishizuka N, Weber J, Amaral D (1990) Organization of intrahippocampal projections originating from CA3 pyramidal cells in the rat. J Comp Neurol *295*:580–623.

Ito M (1984) *The cerebellum and neural control.* Raven Press.

Jaffe D, Johnston D, Lasser-Ross N, Lisman J, Miyakawa H, Ross W (1992) The spread of Na+ spikes determines the pattern of dendritic Ca^{2+} entry into hippocampal neurons. Nature *357*:244–246.

Johnston D, Spruston N (1992) Perforated patch-clamp analysis of the passive membrane properties of three classes of hippocampal neurons. J Neurosci *67*:508–529.

Jonas P, Major G, Sakmann B (1993) Quantal components of unitary EPSCs at the mossy fibre synapse on CA3 pyramidal cells of rat hippocampus. J Physiol (Lond) *472*:615–663.

Kaibara T, Leung LS (1993) Basal versus apical dendritic long-term potentiation of commissural afferents to hippocampal CA1: a current-source density study. J Neurosci *13*:2391–2404.

Katsumaru H, Kosaka T, Heizmann C, Hama K (1988) Immunocytochemical study of GABAergic neurons containing the calcium-binding protein parvalbumin in the rat hippocampus. Exp Brain Res *72*:347–362.

Kawaguchi Y, Hama K (1987) Two subtypes of non-pyramidal cells in rat hippocampal formation identified by intracellular recording and HRP injection. Brain Res *411*:190–195.

Kawaguchi Y, Hama K (1988) Physiological heterogeneity of non pyramidal cells in rat hippocampal CA1 region. Exp Brain Res *72*:494–502.

Kawaguchi Y, Katsumaru H, Kosaka T, Heizmann C, Hama K (1987) Fast spiking cells in rat hippocampus (CA1 region) contain the calcium-binding protein parvalbumin. Brain Res *416*:369–374.

Klapstein G, Colmers W (1993) On the sites of presynaptic inhibition by neuropeptide Y in rat hippocampus in vitro. Hippocampus *3*:103–112.

Knowles W, Schwartzkroin P (1981) Local circuit synaptic interactions in hippocampal brain slices. J Neurosci *1*:318–322.

Knowles W, Traub R, Strowbridge B (1987) The initiation and spread of epileptiform bursts in the in vitro hippocampal slice. Neuroscience *21*:441–455.

Koch C, Zador A (1993) The function of dendritic spines: devices subserving biochemical rather than electrical compartmentalization. J Neurosci *13*:413–422.

Kohonen T (1977) A principal of neural associative memory. Neuroscience *2*:1065–1076.

Kohonen T (1984) *Self-organization and associative memory.* New York: Springer Verlag.

Kosaka T (1980) The axon initial segment as a synaptic site: ultrastructure and synaptology of the initial segment of the rat pyramidal cell in the rat hippocampus (CA3 region). J Neurocytol *9*:861–882.

Kosaka T, Kosaka K, Tateishi K, Hamaoka Y, Yanaihara N, Wu J-Y, Hama K (1985) GABAergic neurons containing CCK-8-like and/or VIP-like immunoreactivities in the rat hippocampus and dendate gyrus. J Comp Neurol *239*:420–430.

Kosaka T, Katsumaru H, Hama K, Wu J-Y, Heizmann C (1987) GABAergic neurons containing the Ca^{2+}-binding protein parvalbumin in the rat hippocampus and dendate gyrus. Brain Res *419*:119–130.

Kosaka T, Wu J-Y, Benoit R (1988) GABAergic neurons containing somatostatin-like immunoreactivity in the rat hippocampus and dentate gyrus. Exp Brain Res *71*:388–398.

Kunkel D, Lacaille J-C, Schwartzkroin P (1988) Ultrastructure of stratum lacunosum-moleculare interneurons of hippocampal CA1 region. Synapse *282*:382–394.

Lacaille J-C (1991) Postsynaptic potentials mediated by excitatory and inhibitory amino acids in interneurons of stratum pyramidale of the CA1 region of rat hippocampal slices in vitro. J Neurophysiol *66*:1441–1454.

Lacaille J-C, Schwartzkroin P (1988a) Stratum lacunosum-moleculare interneurons of hippocampal CA1 region. I. Intracellular response characteristics, synaptic responses, and morphology. J Neurosci *8*:1400–1410.

Lacaille J-C, Schwartzkroin P (1988b) Stratum lacunosum-moleculare interneurons of hippocampal CA1 region. II. Intrasomatic and intradendritic recordings of local circuit synaptic interactions. J Neurosci *8*:1411–1424.

Lacaille J-C, Williams S (1990) Membrane properties of interneurons in stratum oriens-alveus of the CA1 region of rat hippocampus in vitro. Neuroscience *36*:349–359.

Lacaille J-C, Mueller A, Kunkel D, Schwartzkroin PA (1987) Local circuit interactions between oriens/alveus interneurons and CA1 pyramidal cells in hippocampal slices: electrophysiology and morphology. J Neurosci 7:1279–1993.

Lacaille J-C, Williams S, Samulack D, Beaulieu C (1993) Membrane properties of interneurons of stratum lacunosum moleculare in whole cell recordings from rat hippocampal slices. Soc Neurosci Abstr *19*:351.

Lang U, Frotscher M (1990) Postnatal development of nonpyramidal neurons in the rat hippocampus (are CA1 and CA3): a combined Golgi electron microscope study. Anat Embryol (Berl) *181*:533–545.

Laurberg S (1979) Commissural and intrinsic connections of the rat hippocampus. J Comp Neurol *184*:685–708.

Leranth C, Frotscher M (1987) Cholinergic innervation of hippocampal GAD- and somatostatin-immunoreactive commissural neurons. J Comp Neurol *261*:33–47.

Li X-G, Somogyi P, Tepper JM, Buzsáki G (1992) Axonal and dendritic arborization of an intracellularly labeled chandelier cell in the CA1 region of rat hippocampus. Exp Brain Res *90*:519–525.

Li X-G, Somogyi P, Ylinen A, Buzsáki G (1993) The hippocampal CA3 network: an in vivo intracellular labelling study. J Comp Neurol

Liu Y-B, Disterhoft J, Slater N (1993) Activation of metabotropic glutamate receptor induces long-term depression of GABAergic inhibition in the hippocampus. J Neurophysiol *69*:1000–1004.

Lorente de Nó R (1934) Studies of the structure of the cerebral cortex: II. Continuation of the study of the ammonic system. J Psychol Neurol *46*:113–177.

Lytton W, Sejnowski T (1991) Simulations of cortical pyramidal neurons synchronized by inhibitory interneurons. J Neurophysiol *66*:1059–1079.

MacVicar B, Dudek F (1980) Local synaptic circuits in rat hippocampus: interaction between pyramidal cells. Brain Res *184*:220–223.

Madison D, Nicoll R (1988) Enkephalin hyperpolarizes interneurons in the hippocampus. J Physiol (Lond) *398*:123–130.

Major G, Evans J, Back J (1993) Solutions for transients in arbitrary branching cables: I. Voltage recording with a somatic shunt. Biophys J *65*:423–449.

Margerison J, Corsellis J (1966) Epilepsy and the temporal lobes. A clinical, electroencephalographic and neuropathological study of the brain in epilepsy with particular reference to the temporal lobes. Brain *89*:499–530.

McBain C, Dingledine R (1993) Heterogeneity of synaptic glutamate receptors on CA3 stratum radiatum interneurons of rat hippocampus. J Physiol (Lond) *462*:373–392.

McCulloch W, Pitts W (1943) A logical calculus of the ideas immanent in nervous activity. Bull Math Biol *118*:132–136.

Miettinen R, Gulyas A, Baimbridge K, Jacobowitz D, Freund T (1992) Calretinin is present in non-pyramidal cells of the rat hippocampus—II. Co-existence with other calcium binding proteins and GABA. Neuroscience *48*:29–43.

Miles R, (1990) Synaptic excitation of inhibitory cells by single CA3 hippocampal pyramidal cells of the guinea-pig in vitro. J Physiol (Lond) *428*:61–77.

Miles R, Poncer J-C (1993) Metabotropic glutamate receptors mediate a post-tetanic excitation of guinea-pig hippocampal inhibitory neurones. J Physiol (Lond) *463*:461–473.

Miles R, Traub R (1986) Excitatory synaptic interactions between CA3 neurons in the guinea-pig hippocampus. J Physiol (Lond) *373*:397–418.

Miles R, Wong R (1983) Single neurons can initiate synchronized population discharge in the hippocampus. Nature *306*:371–373.

Miles R, Wong R (1984) Unitary inhibitory synaptic potentials in the guinea-pig hippocampus in vitro. J Physiol (Lond) *356*:97–113.

Miles R, Wong R (1987) Inhibitory control of local excitatory circuits in the guinea-pig hippocampus. J Physiol (Lond) *388*:611–629.

Misgeld U, Frotscher M (1986) Postsynaptic GABAergic inhibition of non-pyramidal neurons in the guinea pig hippocampus. Neuroscience *19*:193–206.

Nitsch R, Soriano E, Frotscher M (1990) The parvalbumin-containing nonpyramidal neurons in the rat hippocampus. Anat Embryol (Berl) *181*:413–425.

O'Keefe J (1989) Computation the hippocampus might perform. In: *Neural connections, mental computation* (Nadel L, Cooper L, Culicover P, Harnish R, eds), Cambridge, MA: MIT Press.

O'Keefe J (1990) A computational theory of the hippocampal cognitive map. In: *Progress in brain research*, Vol. 83 (Storm-Mathisen J, Zimmer J, Ottersen O, eds), pp 301–312. New York: Elsevier.

Oleskevich S, Lacaille J-C (1992) Reduction of $GABA_B$ inhibitory postsynaptic potentials by serotonin via pre- and postsynaptic mechanisms in CA3 pyramidal cells of rat hippocampus in vitro. Synapse *12*:173–188.

Patton P, McNaughton B (1993) Towards a computational model of the hippocampal formation incorporating realistic anatomical connectivity. Am Soc Neurosci *19*:795.

Peters A, Jones E (1984) Classification of cortical neurons. In: *Cerebral cortex, vol. 1, cellular components of the cerebral cortex*, Jones E, Peters A, eds), pp 107–121. New York: Plenum Press.

Raastad M, Storm J, Andersen P (1992) Putative single quanbtum and single fibre excitatory postsynaptic currents show similar amplitude range and variability in rat hippocampal slices. Eur J Neurosci *4*:113–117.

Ramón y Cajal S (1911) *Histologie du système nerveux de l'homme et des vertébrés, Tome II.* Paris: Maloine.

Redman S, Walmsley B (1983a) Amplitude fluctuations in synaptic potentials in cat spinal motoneurones in identified group Ia synapses. J Physiol (Lond) *343*:135–145.

Redman S, Walmsley B (1983b) The time course of synaptic potentials evoked in cat spinal motoneurones at identified group Ia synapses. J Physiol (Lond) *343*:117–133.

Ribak C, Vaughn J, Saito K (1978) Immunocytochemical localization of glutamamic acid decarboxylase in neuronal somata following colchicine inhibition of axonal transport. Brain Res *140*:315–332.

Robbins S, Kumar V (1987) *Basic pathology.* Philadelphia: Saunders.

Rolls E (1988) Visual information processing in the primate temporal lobe. In: *Models of visual perception: from natural to artificial* (Imbert M, ed), London: Oxford University Press.

Ropert N, Guy N (1991) Serotonin facilitates GABAergic transmission in the CA1 region of rat hippocampus in vitro. J Physiol (Lond) *441*:121–136.

Rumelhart D, McLelland J (1986) *Parallel distributed processing: explorations in the microstructure of cognition.* Cambridge MA: MIT Press.

Sah P, Hestrin S, Nicoll R (1990) Properties of excitatory postsynaptic currents recorded in vitro from rat hippocampal interneurones. J Physiol (Lond) *430*:605–616.

Samulack D, Lacaille J-C (1991) GABA receptor-mediated synaptic potential in rat hippocampus pyramidal cells elicited by glutamate microapplication at the oriens/alveus border or in stratum pyramidale. Neurosci Abstr *17*:1169.

Samulack D, Lacaille J-C (1993) Hyperpolarizing synaptic potentials evoked in CA1 pyramidal cells by glutamate stimulation of interneurons from the oriens/alveus border of rat hippocampal slices. II. Sensitivity to GABA antagonists. Hippocampus *3*:345–358.

Samulack D, Williams S, Lacaille J-C (1993) Hyperpolarizing synaptic potentials evoked in CA1 pyramidal cells by glutamate stimulation of interneurons from the oriens/alveus border of rat hippocampal slices. I. Electrophysiological response properties. Hippocampus *3*:331–344.

Sayer R (1988) *Synaptic transmission between CA3 and CA1 neurones in the guinea pig hippocampal slice.* Camberra: Australian National University.

Sayer R, Friedlander M, Redman S (1988) Synaptic transmission between individual CA3 and CA1 neurons in the hippocampus. Soc Neurosci Abstr *14*:18.

Sayer R, Redman S, Andersen P (1989) Amplitude fluctuations in small EPSPs recorded from CA1 pyramidal cells in the guinea pig hippocampal slice. J Neurosci *9*:840–850.

Sayer R, Friedlander M, Redman S (1990) The time course and amplitude of EPSPs evoked at synapses between pairs of CA3/CA1 neurons in the hippocampal slice. J Neurosci *10*:826–836.

Schmajuk N, DiCarlo J (1992) Stimulus configuration, classical conditioning, and hippocampal function. Psychol Rev *99*:268–305.

Schmajuk NA, Thieme AD, Blair HT (1993) Maps, routes, and the hippocampus: a neural network approach. Hippocampus *3*:387–400.

Schoepp D, Bockaert J, Sladeczek F (1990) Pharmacological and functional characteristics of metabotropic excitatory amino acid receptors. Trends Pharmacol Sci *11*:508–515.

Schwartzkroin P, Kunkel D (1985) Morphology of identified interneurons in the CA1 region of guinea pig hippocampus. J Comp Neurol *232*:205–218.

Schwartzkroin P, Mathers L (1978) Physiological and morphological identification of a nonpyramidal hippocampal cell type. Brain Res *157*:1–10.

Schwartzkroin P, Prince D (1980) Changes in excitatory and inhibitory synaptic potentials leading to epileptogenic activity. Brain Res *183*:169–181.

Segal M (1990a) A subset of local interneurons generate slow inhibitory postsynaptic potentials in hippocampal neurons. Brain Res *511*:163–164.

Segal M (1990b) Serotonin attenuates a slow inhibitory postsynaptic potential in rat hippocampal neurons. Neuroscience *36*:631–641.

Segev I, Fleshman J, Burke R (1989) Compartmental models of comples neurons. In: *Methods in neuronal modalling* Koch C, Segev I, eds), Cambridge: MIT Press.

Seres L, Ribak C (1983) GABAergic cells in the dendate gyrus appear to be local circuit and projection neurons. Exp Brain Res *50*:173–182.

Sloviter R (1989) Calcium-binding protein (Calbindin-D28k) and parvalbumin immunocytochemistry: localization in the rat hippocampus with specific reference to the selective vulnerability of hippocampal neurons to seizure activity. J Comp Neurol *280*:183–196.

Sloviter R, Nilaver G (1987) Immunocytochemical localization of GABA-cholecystokinin-, vasoactive intestinal polypeptide-, and somatostatin-like immunoreactivity in the area dentata and hippocampus of the rat. J Comp Neurol *256*:42–60.

Somogyi P, Nunzi M, Smith A (1983) A new type of specific interneuron in the monkey hippocampus forming synapses exclusively with the axon initial segments of pyramidal cells. Brain Res *259*:137–142.

Somogyi P, Hodgson A, Smith M, Nunzi A, Gorio A, Wu J-Y (1984) Differential populations of GABAergic neurons in the visual cortex and hippocampus of cat contain somatostatin- or cholecystokinin-immunoreactive material. J Neurosci *4*:2590–2603.

Somogyi P, Freund T, Hodgson A, Somogyi J, Beroukas D, Chubb I (1985) Identified axo-axonic cells are immunoreactive for GABA in the hippocampus and visual cortex of the cat. Brain Res *332*:143–149.

Soriano E, Frotscher M (1993) Spiny nonpyramidal neurons in the CA3 region of the rat hippocampus are glutamate-like immunoreactive and receive convergent mossy fiber input. J Comp Neurol *333*:435–448.

Soriano E, Nitsch R, Frotscher M (1990) Axo-axonic chandelier cells in the rat fascia dentata: golgi-EM and immunocytochemical studies. J Comp Neurol *293*:1–25.

Sorra KE, Harris KM (1993) Occurrence and three-dimensional structure of multiple synapses between individual radiatum axons and their target pyramidal cells in hippocampal area CA1. J Neurosci *13*:3736–3748.

Spruston N, Jaffe D, Williams S, Johnston D (1993) Voltage- and space-clamp errors associated with the measurement of electronically remote synaptic events. J Neurophysiol *70*:781–802.

Squire L (1987) *Memory and brain.* New York: Oxford University Press.

Squire L (1992) Memory and the hippocampus: a synthesis from findings with rats, monkeys, and humans. Psychol Rev *99*:195–231.

Stockley E, Cole H, Brown A, Wheal H (1993) A system for quantitative morphological measurement and electrotonic modelling of neurons: three-dimensional reconstruction. J Neurosci Methods *47*:39–51.

Storm-Mathisen J, Ottersen O (1984) Neurotransmitters in the hippocampal formation. In: *Cortical integration* (Suarez R, Ajmone-Marsan C, eds), pp 105–130. New York: Raven Press.

Swanson L, Wyss J, Cowan W (1978) An autoradiographic study of the organization of intrahippocampal association pathways in the rat. J Comp Neurol *181*:681–715.

Tamamaki N, Nojyo Y (1990) Disposition of the slab-like modules formed by axon branches originating from single CA1 pyramidal neurons in the rat hippocampus. J Comp Neurol *291*:509–519.

Tamamaki N, Nojyo Y (1991) Crossing fiber arrays in the rat hippocampus as demonstrated by three-dimensional reconstruction. J Comp Neurol *303*:435–442.

Tanabe Y, Masu M, Ishii T, Shigemoto R, Nakanishi S (1992) A family of metabotropic glutamate receptors. Neuron *8*:169–179.

Tanabe Y, Nomura A, Masu M, Shigemoto R, Mizuno N, Nakanishi S (1993) Signal transduction, pharmacological properties, and expression patterns of two rat metabotropic glutamate receptors, mGluR3 and mGluR4. J Neurosci *13*:1372–1378.

Thompson S, Capogna M, Scanziani M (1993) Presynaptic inhibition in the hippocampus. Trends Neurosci *16*:222–227.

Thomson A, Radpour S (1991) Excitatory connections between CA1 pyramidal cells revealed by spike triggered averaging in slices of rat hippocampus are partially NMDA receptor mediated. Eur J Neurosci *3*:587–601.

Traub R, Miles R (1991) *Neuronal network of the hippocampus.* New York: Cambridge University Press.

Traub R, Miles R, Wong R (1987a) Models of synchronized hippocampal bursts in the presence of inhibition. I. Single population events. J Neurophysiol *58*:739–751.

Traub R, Miles R, Wong R, Schulman L, Schneiderman J (1987b) Models of synchronized hippocampal bursts in the presence of inhibition. II. Ongoing spontaneous events. J Neurophysiol *58*:752–764.

Traub RD, Wong RKS, Miles R, Michelson H (1991a) A model of CA3 Hippocampal pyramidal neuron incorporating voltage-clamp data on intrinsic conductances. J Neurophysiol *66*:635–650.

Traub RD, Wong RKS, Miles R, Michelson H (1991b) A model of CA3 hippocampal pyramidal neuron incorporating voltage-clamp data on intrinsic conductances. J Neurophysiol *66*:635–650.

Traub RD, Miles R, Buzsaki G (1992a) Computer simulation of carbachol-driven rhythmic population oscillations in the CA3 region of the in vitro rat hippocampus. J Physiol (Lond) *451*:653–672.

Traub RD, Miles R, Jefferys JGR (1992b) Simulation and experimental analysis of an epileptic oscillation in the in vitro hippocampal slice. Am Soc Neurosci *18*:1240.

Traub RD, Miles R, Jefferys JGR (1993a) Synaptic and intrinsic conductances shape picrotoxin-induced synchronized after-discharges in the guinea-pig hippocampal slice. J Physiol (Lond) *461*:525–547.

Traub RD, Miles R, Jefferys JGR (1993b) Synaptic and intrinsic conductances shape picrotoxin-induced synchronized after-discharges in the guinea-pig hippocampal slices. J Physiol (Lond) *461*:525–547.

Treves A, Rolls E (1992) Computational constraints suggest the need for two distinct input systems to the hippocampal CA3 network. Hippocampus *2*:189–200.

Treves A, Miglino O, Parisi D (1992) Rats, nets, maps, and the emergence of place cells. Psychobiology *20*:1–8.

Turner D (1988) Waveform and amplitude characteristics of evoked responses to dendritic stimulation of CA1 guinea-pig pyramidal cells. J Physiol (Lond) *395*:419–439.

Turner R, Meyers D, Richardson T, Barker J (1991) The site for initiation of action potential discharges over the somatodendritic axis of rat hippocampal CA1 pyramidal neurons. J Neurosci *11*:2270–2280.

Turner RW, Meyers DER, Barker JL (1993) Fast pre-potential generation in rat hippocampal CA1 pyramidal neurons. Neuroscience *53*:949–959.

Voronin L, Kuhnt U, Hess G, Gusey A, Roschin V (1992) Quantal parameters of "minimal" excitatory postsynaptic potentials in guinea pig hippocampal slices: binomial approach. Exp Brain Res *89*:248–264.

Wenzel J, Kirshe W, Kunz G, Neumann H, Wenzel M, Winkelmann E (1962) Licht- und elektronenmikroskopische Untersuchungen uber die Dendritenspines an Pyramiden-Neuronen des Hippocampus (CA1) bei der Ratte. J Hirnforsch *13*:387–408.

Westrum L, Blackstad T (1962) An electron microscopic study of the stratum radiatum of the rat hippocampus (regio superior, CA1) with particular emphasis on synaptology. J Comp Neurol *119*:281–292.

Williams S, Johnston D (1991) Kinetic properties of two anatomically distinct excitatory synapses in hippocampal CA3 pyramidal neurons. J Neurophysiol *66*:1010–1020.

Williams S, Lacaille J-C (1992) $GABA_B$ receptor-mediated inhibitory postsynaptic potentials evoked by electrical stimulation and by glutamate stimulation of interneurons in *stratum lacunosum-moleculare* in hippocampal CA1 pyramidal cells in vitro. Synapse *11*:249–258.

Williams S, Lacaille J-C (1993) Synaptic responses of interneurons of stratum lacunosum-moleculare in whole cell recordings from rat hippocampal slices. Soc Neurosci Abstr *19*:351.

Willis J, Ge Y, Wheal H (1993) Simulation of hippocampal epileptiform activity using transputers. J Neurosci Methods *47*:205.

Willis JB, Ge YC, Wheal HV (1993) Simulation of epileptiform activity in the hippocampus using transputers. J Neurosci Methods *47*:205–213.

Wong RKS, Stewart M (1992) Different firing patterns generated in dendrites and somata of CA1 pyramidal neurones in guinea-pig hippocampus. J Physiol (Lond) *457*:675–687.

Wong R, Prince D, Basbaum A (1979) Intradendritic recordings from hippocampal neurons. Proc Natl Acad Sci USA *76*:986–990.

Woodson W, Nitecka L, Ben-Ari Y (1989) Organization of the GABAergic system in the rat hippocampal formation: a quantitative immunocytochemical study. J Comp Neurol *280*:254–271.

Xie X, Smart TG (1993) Properties of GABA-mediated synaptic potentials induced by zinc in adult rat hippocampal pyramidal neurones. J Physiol (Lond) *460*:503–523.

APPENDIX A

All the numerical values given hereafter are parameters which may be changed by the modeler in the routines described in Appendix B. In the following we used these abbreviations: PC, pyramidal cell; I, interneuron; SO, stratum oriens; SR, stratum radiatum; S, septal; T, temporal; pa, probability of activation; pc, probability of finding a connection.

General anatomical considerations

According to our own measurements the following distances can be used: L_CA3 = 2.4 mm for the transverse length of CA3 area and L_CA1 = 1.7 mm for the transverse length of CA1 area in the central part along the septo-temporal axis and T_S = 400 μm for the depth of a typical slice. A length of T_S = 8.0 mm can be used to model CA3 and CA1 areas along the whole extent of the longitudinal axis.

APPENDIX A1. Number and Spatial Distribution of Hippocampal Neurons in a Slice

Cell type	Total number	Number along transverse axis	Number in slice depth	Inside stratum pyramidale thickness
CA3 pyramidal	9,680	121	20	4
CA3 chandelier	40	20	2	
CA3 basket	180	30	6	
CA3 oriens	180	30	6	
CA1 pyramidal	15,930	118	27	5
CA1 chandelier	39	13	3	
CA1 O/A	203	29	7	
CA1 basket	203	29	7	
CA1 L-M	203	29	7	

APPENDIX A2. Characteristics of Schaffer/Commissural Projections

Emitting CA3 PCs	Locus of projection	Orientation	PC synapses	I synapses
Proximal	Distal SO and SR	S 15°	150 μV: pa=0.1, pc=0.06; AMPA only	300 μV: pa=0.1, pc=0.06 NMDA/AMPA (25%/75%)
Mid	Mid SO and SR	S and T	Id	Id
Distal	Distal SR	T 22°	Id	Id

APPENDIX A3. CA3 Associational Pathway

Emitting CA3 PCs	Projection Area	Orientation	PC synapses	I synapses
Proximal	Local SO and SR	Ratio S/T=3	1.4 mV: pa=0.85, pc=0.02 70% AMPA 30% NMDA	1.9 mV: pa=0.85, pc=0.1; AMPA for non SR I, 80 % AMPA and 20% NMDA for 75% of SR I, NMDA for the rest
Mid	All directions SR	S and T	Id	Id
Distal	Backward SO	Ratio S/T=1/3	Id	Id

APPENDIX A4. Patterns of Connectivity of CA3 Inhibitory Interneurons

Emitting CA3 I	Locus of projectin	Orientation	PC synapses	I synapses
Chandelier cell	Initial segment of CA3 pyramidal cells	Ellipsoidal field	Hinders spiking during a fixed time window: pa=1.0, pc=0.29	on SR I: pa=1.0, pc=0.29
SO I	Soma of all CA3 neurons	Ellipsoidal field	2.2 mV $GABA_A$: pa=0.1, pc=0.6	2.2 mV $GABA_A$: pa=1.0, pc=0.2
SR I	Soma of all CA3 neurons	Ellipsoidal field	2.2 mV $GABA_A$: pa=0.1, pc=0.6	2.2 mV $GABA_A$; pa=1.0, pc=0.2

APPENDIX A5. CA1 Associational pathway

Emitting CA1 PCs	Locus of projection	Orientation	PC synapses	I synapses
Proximal	SO with fan out of 90°	S and T	AMPA 0.1 mV, NMDA 0.2 mV: pa=0.8, pc=0.007	AMPA 0.7 mV, NMDA 1.5 mV pa=0.7, pc=0.3 for baskset I, pc=0.64 for O/A I
Mid	As proxial with surrounding local field	Id	Id	Id
Distal	Backward SR	Id	d	Id

APPENDIX A6. Patterns of Connectivity of CA1 Inhibitory Interneurons

Emitting CA1 I	Locus of projection	Orientation	PC synapses	I synapses
Chandelier cell	Initial segment of CA1 PCs	Ellipsoidal field	Hinders spiking during a fixed time window: pa=1.0, pc=0.13	On Basket cells same action as on PCs pa=1.0, pc=0.2
SO I	Soma of all CA1 neurons	Id	2.2 mV $GABA_A$: pa=1.0, pc=0.6	2.2 mV $GABA_A$: pa=1.0, pc=0.2
SR I	Soma of all CA1 neurons	Id	2.2 mV $GABA_A$: pa=1.0, pc=0.6	2.2 mV $GABA_A$: pa=1.0, pc=0.2
L-M I	Dendritic tree of all neurons	Id	0.91 mV in the soma, 0.67 mV in the dendrites $GABA_A/GABA_B$: pa=0.5, pc=0.64	0.91 mV on Basket cells: pa=0.5, pc=0.5, $GABA_A/GABA_B$

APPENDIX B

All programs are written in standard C and can be run on any machine. They are available on request. Our simulations were run on a Silicon Graphics Crimson, and colour figures were obtained using the software Explorer.

Connectivity matrix between CA3 and CA1: program CA31

This program constructs the connectivity matrix between CA3 pyramidal cells (for the Schaffer collaterals and the commissural fibres) and the different types of neurons in CA1 (pyramidal cells and inhibitory interneurons). The different parameters are G, G31_1, G31_2, G31_3, p31, and those listed in Appendix A, i.e., the different lengths and number of neurons along the different axes. G is the parameter which controls the dispersion of the Gaussian distribution used to determine the locus of projection in CA1 dendritic trees. The random number generator we use is not biased since it is built following the Starcenko theorem which guarantees a uniform distribution in the hypercube of infinite dimension (Bernard et al., 1993). G31_1 controls the dispersion of the Gaussian distribution used to calculate the angle of the Schaffer collaterals with respect to the transverse axis. G31_2 and G31_3 control the dispersion of the Gaussian distribution along the I and J axes. p31 is the probability that the afferent fibre contacts a given CA1 neuron.

Each CA3 pyramidal cell is given a value: 0, 1, or 2. These figures represent the locus of projection in CA1, i.e., upper radiatum, lower radiatum + upper oriens and lower oriens, respectively. The repartition is done as follows: The CA3 area is separated in two equal zones in the transverse direction. CA3 pyramidal cells in the first zone (proximal in respect to the dentate gyrus) have a probability to get the 0 value according to their transverse location. The distribution is Gaussian (using G as a parameter) centred on the border with the dentate gyrus (i.e., the most proximal CA3 pyramidal cells) with an obvious probability = 1.0 at this locus to get the 0 value. The third zone is the inverted image of the first one, the most distal CA3 pyramidal cells (next to CA1) have a probability = 1.0 to get the 2 value. All the other CA3 pyramidal cells get the 1 value.

Each CA3 efferent fibre (Schaffer collateral or commissural fibre) is then given its orientation in the longitudinal direction (random Gaussian distribution) with obvious probability of 1.0 to be in the septal (temporal) direction for most proximal (distal) CA3 pyramidal cells and 0.5 in either direction for mid cells. The angle relative to the transverse axis is taken from a random Gaussian distribution around a central value calculated from the maximum values of $+15°$ and $-22°$ at both borders of the CA3 area. This central value decreases linearly along the transverse axis between those two limits.

The point where the maximum density of terminals can be found (X_{max}, Y_{max}) is computed. We then build the probability matrix (g_{ij}) with $g_{ij} = g_1 \times g_2$, where $g_1 = \exp(-(X_{max}-i)^2/2 \times G31\_2^2)$ and $g_2 = \exp(-(Y_{max}-j)^2/2 \times G31\_3^2)$.

(X_{max}, Y_{max}) in the central element of this matrix with obviously $g_{X_{max}Y_{max}} = 1.0$.

The matrix is then rotated so as to align its rows with the I axis. Once this area of possible contacted neurons computed we apply the probability of an effective link p31 $\times$ g_{ij} for CA1 neurons which coordinates are (i,j) in the new set of coordinates (I and J axes). If the neuron is contacted its coordinates are stored in a relevant file, together with the location of the synapse (i.e., 0, 1, or 2), the synaptic weight (i.e., a value taken from a random Gaussian distribution centred on 150 μV), the probability of activation of the synapse (i.e., a value taken from a random Gaussian distribution centred on 0.1), and the ratio of NMDA and AMPA receptors.

Connectivity matrix from CA3 pyramidal cells to CA3 neurons: program CA33

This program constructs the connectivity matrix between CA3 pyramidal cells and the different types of neurons in CA3 (pyramidal cells and inhibitory interneurons). The different parameters are G, G33_1, G33_2, G33_31, G33_32, p33, and those listed in Appendix A. As in the program described above each CA3 pyramidal cell is given a value: 0, 1, or 2. These figures represent the locus of projection in CA3. Zero corresponds to cells obeying a proximal connectivity rule with a septal extension 3 times bigger than the temporal one, 1 for cells obeying the mid connectivity rule with a septal extension similar to the temporal one and 2 for cells projecting backward with a temporal extension three times bigger than the septal one. The distribution is controlled by the dispersion parameter G. G33_1 and G33_2 control the dispersion of the Gaussian

distribution used to build the connectivity matrix along the I axis toward the septal and temporal ends, respectively. Along J axis the parameter G33_3(i) controlling the dispersion of the Gaussian distribution varies between G33_31 and G33_32 for the most proximal and distal cells respectively.

We take G33_3(i) = G33_32 − (G33_32-G33_31) × exp(−i^2/200).

The point where the maximum density is then computed and the connectivity matrix is built with g_{ij} = G33_3(i) × exp (−(Y_{max}−j)^2/2 × G33_2^2) for j ≥ Y_{max} and g_{ij} = G33_3(i) × exp (−(Y_{max}−j)^2/2 × G33_1^2) otherwise.

For each cell type the probability of connection is then applied, i.e., p33 × g_{ij}. If the neuron is contacted its coordinates are stored in a relevant file, together with the location of the synapse (i.e., 0, 1, or 2) and the synaptic weight (i.e., a value taken from a random Gaussian distribution centred on 1.4 mV, with 30% NMDA and 70% non-NMDA component) for pyramidal cells. For all interneurons the distribution of EPSP amplitudes is centred on 1.9 mV. Chandelier cells and stratum oriens interneurons are supposed to have non-NMDA receptors only, whereas 75% of the stratum radiatum interneurons have a mixture of both AMPA (80%) and NMDA (20%) receptors and the other 25% have a special kind of non-NMDA receptor with long-duration response and inward rectifying current. The repartition of these two types of stratum radiatum interneurons is taken randomly. The probability of activation of synapses on pyramidal cells and interneurons is given an average value of 0.85 (Gaussian distribution centred on 0.85).

Connectivity matrix from CA1 pyramidal cells to CA1 neurons: program CA11

This program constructs the connectivity matrix between CA1 pyramidal cells and the different types of neurons in CA1 (pyramidal cells and inhibitory interneurons). The different parameters are G, p11 and those listed in Appendix A. As in the previous section each CA1 pyramidal cell is given a value—0, 1, or 2—with G11 controlling the dispersion of the Gaussian distribution. These figures represent the pattern of connectivity of CA1 pyramidal cells. Zero corresponds to proximal cells projecting toward the subiculum with a certain probability, 1 for cells obeying the mid connectivity rule with a circular local pattern of connectivity and a more diffuse one toward the subiculum (one probability for each pattern), and 2 for cells projecting backward with a certain probability. To take into account the septotemporal gradient each cell projects in a fan out fashion (45° in septal and temporal directions). The dispersion of the distribution is controlled by G. Type 0 and type 1 cells project into the stratum oriens (−1) and type 2 cells project distally in the stratum radiatum. EPSPs amplitudes are given Gaussian distributions centred around the values corresponding at each class of contacted neuron as listed in Appendix A4. The synaptic weight is centred on 0.2 mV for the NMDA component and 0.1 mV for the non-NMDA component for pyramidal cells. For all interneurons the distribution of EPSP amplitudes is centred on 1.5 mV and 0.7 mV, respectively. For all populations the probability of activation of the synapse is given a value centred on 0.8 (Gaussian distribution).

Connectivity matrix from interneurons to pyramidal neurons: program Inter

This program constructs the connectivity matrix between all interneurons and all pyramidal cells in both CA1 and CA3 areas. Each subset of interneurons and pyramidal cell is treated separately. The different parameters are GIE_1, GIE_2, A, B, pIE, and those listed in Appendix A.

Each interneuron is given a possible elliptical connectivity field. The long and short axes are calculated from peaked Gaussian distribution centred around A and B, respectively. A and B are aligned along the longitudinal and transverse axes, respectively. Obviously if one wishes a greater extension along the transverse axis it is sufficient to take B>A. GIE_1 and GIE_2 control the dispersion of the Gaussian distributions used to build the connectivity matrix (same as in the previous sections). The probability of connection between the interneuron and the pyramidal cell located in its field is then applied, i.e., pIE × g_{ij}.

The other parameters are given values distributed around the ones listed in Appendix A3 and A5.

APPENDIX C

Progress in the understanding of the structure and function of hippocampal neurones and their networks is fast moving. While this manuscript was in press, important new anatomical and electrophysiological data related to the CA3 and CA1 areas were reported. With the editors' approval, we have added this appendix which contains these recent developments. They seem particularly important since they further stress the heterogeneity of neurons in these regions of the hippocampus.

CA3 interneurons have been better characterized. In particular, it has been reported that glutamate-immunoreactive interneurons located below the CA3 stratum pyramidale also receive mossy fibre inputs. Asymmetric synapses are located on horizontal cells, which themselves are sparsely distributed since only five to eight can be found in a slice. The axon of this cell is distributed in stratum radiatum but its exact 3D projection remains to be determined (M. Frotscher, personal communication).

Dentate and CA1 axo-axonic cells have been recently characterized both anatomically and electrophysiologically (see below), although their existence in the CA3 region has not yet been proven. However, they have been found in Golgi studies (M. Frotscher, personal communication). These observations help to justify their presence in the connectivity model. Furthermore, until they are characterized electrophysiologically it seems reasonable to use the data derived from the recordings made in the CA1 region.

To further compound the complexity of interactions between cells it has been reported that following antagonism of NMDA, AMPA, and $GABA_A$ receptors, a giant $GABA_B$ receptor-mediated response has been recorded from pyramidal cells. The data suggests that these events were generated by a subpopulation of interneurones which exhibited bursting activity through electrotonic coupling at gap junctions (H. Michelson, personal communication). However, neither the class of interneuron nor the gap juctions have yet been clearly identified.

Further detail is emerging on the pattern of connectivity between interneurons in the CA1 region. The somata of VIP-

immunoreactive interneurons have been located in the stratum pyramidale of CA1, whose axonal arborization may extend in stratum pyramidale, radiatum, and oriens/alveus. Those that project to the stratum oriens/alveus seem to solely contact somatostatin-immunoreactive interneurons. They are thus highly specialised neurons since they control the activity of GABAergic neurons alone. Furthermore, those VIP neurons with an axonal arbor terminating in the stratum radiatum contact solely GABAergic neurons which are somatostatin immunonegative (T. Freund, personal communication).

Basket cells have been shown to have multiple release sites on CA1 pyramidal cells, whereas the reciprocal projections have a only a single release site. Following suppression of slow $GABA_B$-mediated inhibition there is an increase in the amplitude of the fast IPSPs recorded in CA1 pyramidal cells. Under these conditions, some pyramidal cells exhibit a postinhibitory rebound following the IPSP. This rebound may in turn elicit the discharge of the CA1 pyramidal cell (Buhl et al., 1994). From a functional point of view this is an important result since it suggests that despite the strong inhibitory shunt generated by the basket cells, there may be a period of hyperexcitability of the pyramidal cells.

Progress has also been made in the understanding of the connectivity and behaviour of axo-axonic cells. Only half of the interneurons in CA1 which synapse on the initial segment have all their synapses on this specialised region of the pyramidal cells. The other interneurons may have from 10 to 100% of their synaptic connectivity on the initial segment. Furthermore, there are many axonal branches in the vicinity of the initial segment which do not contribute to these axo-axonic synapses. This result has been described in Wistar rats only and is at odds with previous reports in cats and monkeys (P. Somogyi, personal communication). Physiological properties of axo-axonic neurons have also been characterized recently. There are fast spiking cells, which show adaptation and whose response to the activation of the Schaffer collaterals pathway is mainly mediated through non-NMDA receptors (Buhl et al., 1994).

Finally, a class of interneurons was identified in the oriens/alveus layer of the CA1 region with extensive projection to all major hippocampal regions. These are fast spiking interneurons with morphological characteristics of the NADPH-diaphorase and somatostatin neurons. Since they produce nitric oxide, their hypothesized function is to allow plastic changes in the dentate–CA3-CA1 excitatory circuit that leads to the activation of these neurons. They form 22,000 boutons and the total axon length is 120 mm with a 2.8 mm septo-temporal extent (Penttonen et al., 1994).

Interneurons in both CA3 and CA1 areas seem thus to be extremely heterogenous. Moreover, the discovery of an inhibitory neuron connecting the dentate gyrus and the CA3 and CA1 areas may be functionally very important. We have hypothesized in the discussion that a spatially and temporally restricted activation of excitatory inputs may create a local area of excitation surrounded by a large halo of inhibition. A similar result has been recently reported in the dentate gyrus where restricted, local application of bicuculline produced multiple discharges when recorded locally but gave rise to a widespread area of inhibition in both longitudinal and transverse directions (Sloviter and Brisman, 1994).

We have previously mentioned that we had not included a role for metabotropic receptors in our model, since very few data were available about their 3D location. Moreover, the functional consequences of their activation still needs to be better elucidated before incorporating them into the model. However, ACPD, a metabotropic receptor agonist, has been shown recently to induce rhythmic depolarisations in some oriens/alveus CA1 interneurons. This rhythmic activity continues even after the application of ACPD has stopped. These interneurons essentially project to the lacunosum-moleculare region. Other oriens/alveus interneurons which project to stratum pyramidale do not show this rhythmicity following the application of ACPD. However, in elevated K^+ medium, CA3 pyramidal cells show spontaneous activity locked with that of the oriens interneurons, suggesting a common set of afferents. The putative metabotropic receptor antagonist MCPG reduces the rhythmicity but does not affect the excitability of the cells (McBain et al., 1994). However, it is not known if these interneurons belong to another already characterized Oriens/Alveus interneuron subclass or whether they constitute a class of their own.

Finally, although we have not included entorhinal inputs in the model, recent results seem to indicate that they may play an important and complex role in the processing of information converging on CA1 pyramidal cells and interneurons. Synapses made by perforant path are located on spines, and both NMDA and AMPA subsets of receptors can be activated. Activation of this pathway does not result in the firing of pyramidal cells, probably owing to the coactivation of inhibitory pathways. However, although its action on interneurons remains to be elucidated, it has been proposed that its role would be to boost excitatory inputs in the stratum radiatum (Levy and Colbert, 1992; Colbert and Levy, 1992a,b). Furthermore, different patterns of stimulation of the perforant path may lead to monosynaptic and polysynaptic long-term potentiation in areas CA1 and CA3 (M. Yeckel, personal communication).

REFERENCES

Buhl E, Halasy K, Somogyi P (1994) Nature (in press).

Buhl E, Lovinczi Z, Strezhka V, Karnup S, Somogyi P (1994) Physiological properties of axo-axonic cells in the hippocampus. J Neurophysiol (in press).

Colbert C, Levy W (1992a) Electrophysiological and pharmacological characterization of perforant path synapses in CA1: mediation by glutamate receptors. J Neurophysiol 68:1–8.

Colbert C, Levy W (1992b) GABA-A inhibition opposes monosynaptic perforant path excitation of CA1 pyramids. Soc Neurosci Abstr 18:1496.

Levy W, Colbert C (1992) Associative potentiation of Schaffer collaterals by paired conditioning with the perforant path in hippocampal CA1. Soc Neurosci Abstr 18:1496.

McBain C, Okhiara T, Kauer J (1994) Activation of metabotropic glutamate receptors differentially affects two classes of hippocampal interneurons and potentiates excitatory transmission. J Neurosci 14 (in press).

Penttonen M, Sik A, Ylinen A, Buzsaki G (1994) Widespread inhibitory CA1-CA3-dentate gyrus backprojection in the hippocampus. Soc Neurosci Abstr (in press).

Sloviter B, Brisman B (1994) Epilepsia (in press).